Title: IL-10 driven memory T cell survival and Tfh differentiation promote HIV persistence

*Susan Pereira Ribeiro[1], *Malika Aid[2], *Frank P. Dupuy[3], Chi Ngai Chan[4], Judd Hultquist[5,9], Claire Delage[6], Eirini Moysi[7], Deanna Kulpa[8], Lianghzu Li[1], Xuan Xu[1], Banumathi Tamilselvan[1], Jeffrey Tomalka[1], Michael Nekorchuk[4], Kathleen Busman-Sahay[4], Rebeka Bordi[1], Camille Simoneau[9], Jean Philippe Goulet[10], Vincent Marconi[11,12], Jean Pierre Routy[13], Robert Balderas[14], Luca Micci[15], Bonnie Howell[15], Dan H. Barouch[2], Nevan Krogan[9,17], Constantinos Petrovas[7], Mirko Paiardini[16], Steven G Deeks[18], Jacob D. Estes[4], Daniel Gorman[15], Daria Hazuda[15], #Rafick Pierre Sekaly[1]

* Authors contributed equally

Affiliations

1. Center for System Immunology, Department of Pathology, School of Medicine, Case Western Reserve University, Cleveland, OH, 44106, USA.
2. Center for Virology and Vaccine Research, Beth Israel Deaconess Medical Center, Harvard Medical School, Boston, MA, 02215, USA.
3. Centre hospitalier de l'Université de Montréal, Montreal, QC, H2X 3E4, Canada
4. Vaccine and Gene Therapy Institute, Oregon Health and Science University, Portland, OR, 97006, USA.
5. Division of Infectious Diseases, Northwestern University Feinberg School of Medicine, Chicago, IL, 60611, USA.
6. AIDS and Cancer Virus Program, Frederick National Laboratory for Cancer Research, Leidos Biomedical Research Inc., Frederick, MD, 21701, USA.
7. Immunology Laboratory, Vaccine Research Center, NIAID, NIH, Bethesda, MD, 20814, USA.
8. Department of Pediatrics, Department of Pathology and Laboratory Medicine, Emory University School of Medicine, Atlanta, GA, 30322, USA.
9. Gladstone Institutes, San Francisco, CA, 94158, USA;
10. Caprion Biosciences Inc., Montreal, QC, H2X 3Y7, Canada;
11. Division of Infectious Diseases, Emory University School of Medicine. Atlanta, GA.
12. Emory Vaccine Center, Rollins School of Public Health, Emory University, Atlanta, GA. USA., Atlanta VA Medical Center. Decatur, GA, 30322, USA;
13. Chronic Viral Illness Service, Division of Hematology, McGill University Health Centre, 1001 Blvd Décarie, Montréal, QC, H4A 3J1, Canada;

14. Becton Dickinson, San Diego, CA, 92130, USA.
15. Merck & Co., Inc., Kenilworth, NJ, 07033, USA.
16. , Inc., Kenilworth, NJ, , USA.
17. Emory Vaccine Center and Yerkes National Primate Research Center, Department of Pathology and Laboratory Medicine, Emory University, School of Medicine, Atlanta, GA, 30329, USA.
18. Department of Microbiology, Icahn School of Medicine at Mount Sinai, New York, NY, 10029, USA;
19. Division of HIV, Infectious Diseases, and Global Medicine, University of California, San Francisco, San Francisco, CA, USA.

[#]Corresponding Author: Rafick P. Sekaly - rafick.sekaly@case.edu

Footnote

Further information and requests for resources and reagents should be directed to and will be fulfilled by the Lead Contact, Rafick P. Sekaly (rafick.sekaly@case.edu)

Summary

Mechanisms regulating HIV persistence are complex and not well understood. Increased IL-10 levels were positively associated with HIV reservoir in blood and lymph nodes (LN) of treated HIV aviremic individuals. In LNs, B cells, regulatory T cells, follicular T helper cells (Tfh), monocytes and macrophages contributed to the frequencies of IL10+ cells. Cells with HIV DNA in LNs were in close proximity to IL-10+ cells and/or had the active form of STAT3, the transcription downstream of IL-10. Gene signatures and proteins associated to cell survival, Co-inhibitory receptors expression, maintenance of memory T cells, immune metabolism and Tfh frequencies were all modulated by IL-10 and associated with HIV reservoir persistence. *In vitro,* STAT3 knockout or neutralization of IL-10, reverted all the aforementioned pathways and resulted in 10-fold decay in HIV reservoir. Collectively, these results provide strong evidence for a pivotal role of IL-10 in HIV persistence, and a potential therapeutic strategy for HIV cure.

Keywords: HIV-persistence, IL-10, survival, Co-inhibitory receptors, Tfh cells, IL-10-blockade, STAT3-KO

Introduction

HIV infection triggers a cascade of cytokine production commonly referred as cytokine storm(McMichael et al., 2010, Brockman et al., 2009). Sensing of the virus by PRRs (Pattern recognition receptors)(Jakobsen et al., 2015, Decalf et al., 2017, Hertoghs et al., 2017) and concomitant early gastrointestinal tract barrier damage ensuing bacterial translocation boosts generalized inflammation and immune activation. Importantly, the sensing of bacterial products by TLRs can trigger IL-10

production(Zevin et al., 2016), a pleiotropic anti-inflammatory cytokine(Rojas et al., 2017) that is dramatically increased within weeks of the onset of HIV and SIV infections(McMichael et al., 2010, Estes et al., 2006). IL-10 is produced by several innate immune cell subsets (monocytes, macrophages, dendritic cells) and B cells downstream of the activation of PRRs including TLRs(Kubo and Motomura, 2012). T regulatory cells (Tregs) and Type I regulatory cells (Tr1) also produce IL-10 upon TCR engagement(Shive et al., 2015). IL-10 impedes crucial APC functions by inhibiting cytokine production and preventing the upregulation of Major Histocompatibility Complex (MHC) and co-stimulatory molecules(Mittal and Roche, 2015, Rojas et al., 2017). IL-10 also acts directly on T cells by inhibiting tyrosine phosphorylation downstream of CD28 signaling in T cells(Taylor et al., 2007), decreasing their proliferation, differentiation, and cytokine production (IL-2/IFNg). Several members of the Herpes virus family including CMV, EBV and others encode for IL-10 analogs and as a result, these viruses evade the immune response by inducing peripheral tolerance and promote their own survival(Weber-Nordt et al., 1996) and persist for life in infected hosts(Herbein, 2018, Jochum et al., 2012, Avdic et al., 2011, Slobedman et al., 2009). Hence in LCMV infection, production of IL-10 correlates with poor pathogen control(Kahan and Zajac, 2019); experimental ablation of IL-10 or inhibition of IL-10 signaling restores pathogen control and reduces the severity of disease(Couper et al., 2008). Furthermore, in HIV infected individuals, IL-10 is known to inhibit CD4 and CD8 T cell proliferation and cytokine production *in vitro*; blockade of IL-10 efficiently restored these functions in both HIV and HCV infected individuals *in vitro* (Brockman et al., 2009,

Clerici et al., 1994, Landay et al., 1996, Wilson and Brooks, 2011, Cacciarelli et al., 1996, Rigopoulou et al., 2005, Yang, 2009).

HIV integrates into the host genome and persists in a small pool of long-lived or proliferating memory CD4 T cells(Lee and Lichterfeld, 2016, Murray et al., 2016, Persaud et al., 2000). Low levels of viral transcription/translation and molecular mechanisms that maintain the survival of productively infected cells facilitate the persistence of the HIV reservoir in the host(Chomont et al., 2009). Latently infected cells are known to express high levels of co-inhibitory receptors, such as PD-1, LAG-3, TIGIT and CTLA4(Fromentin et al., 2016, Chomont et al., 2009, Fromentin et al., 2019, McGary et al., 2017). Follicular T helper cells (Tfh) in B cell follicles also contribute to the formation and maintenance of the HIV reservoir, as they harbor quantitatively more intact provirus(Perreau et al., 2013) than non-Tfh cells. Of note, B cells which produce IL-10 are dependent on IL-10 for their own survival(McGary et al., 2017), and are critical for the maintenance of Tfh frequencies(Kerfoot et al., 2011). *Little is known about the role that IL-10 plays in the establishment and the maintenance of HIV reservoir size. Herein, we used unbiased holistic approaches, including tissue in situ, ex vivo, and in vitro experimental methodologies to identify and mechanistically interrogate the interplay between IL-10 and HIV persistence in infected patients.*

RESULTS

Significantly increased levels of circulating IL-10 in treated HIV infected individuals (aviremics) is associated with the size of latent HIV reservoir. In

plasma from antiretroviral (ART) treated HIV aviremic individuals (n=24) and HIV negative healthy controls (HC, n=4) (subgroup representative of a larger cohort, **Table S1**), 23 cytokines (IFN-2a, IFN-b, IFN-g, IL-10, IL-15, IL-17A, IL-18, IL-1b, IL-2, IL-21, IL-22, IL-27, IL-29, IL-33, IL-4, IL-6, IL-7, IL-8, IL-9, TNF-a, TGF-b1, TGF-b2 and TGF-b3) were evaluated using the Meso-Scale platform (MSD). IL-10 was the only cytokine with significantly higher levels in HIV aviremic individuals when compared to HIV negative healthy individuals [Median HIV-aviremics: 455 fg/mL, fold change (FC) HIV/HC: 1.4, $p<0.05$] (**Fig S1a and Fig 1a**) that was also positively correlated with the frequencies of circulating latently infected cells as measured by HIV integrated DNA (HIV IntDNA), a well-accepted readout for HIV reservoir(Eriksson et al., 2013) (Median HIV-aviremics: log 2.85 cps/10^6 CD4 T cells, $p<0.05/r=0.44$ – **Fig S1b and Fig 1b**). None of the other cytokines known to trigger the transcription factor (TF) STAT3(Donnelly et al., 1999), such as IL-9, IL-6, IL-21, IL-22, IL-27(Demoulin et al., 1996, Hillmer et al., 2016), were increased or associated with HIV IntDNA in this cohort (**Fig S1a** and **b**, respectively). The potential role of IL-10 in the persistence of HIV was further supported by the heightened per cell expression of the IL-10 receptor (judged by Mean Fluorescence Intensity - MFI) in different memory CD4 T cell subsets from HIV aviremic as compared to HIV negative healthy individuals (Median MFI IL-10Ra Total CD4 HIV-aviremics: 6167, FC HIV/HC: 1.2, $p=0.003$ - **Fig. S1c**) as measured by flow cytometry. The per cell level of IL10Ra expression in CD45RA+ cells (a cell subset that includes T stem cell memory (TSCM), a target for HIV infection(Chahroudi et al., 2015)), was also positively associated with HIV IntDNA

reservoir (p<0.03/ r= 0.37 - Pearson Correlation **- Fig. S1d)**. It is important to highlight that no other clinical parameter was associated with HIV reservoir in this study (time of HIV infection: median: 7.5 years – p = 0.70, r = -0.07; age: median: 50.5 years old - p = 0.75, r = -0.06; time under ART: median: 3 years - p = 0.34, r = -0.16; CD4 nadir: median 251 cells/mL - p = 0.31, r = -0.17; CD4 counts: median 446 cells/mL - p = 0.25, r = -0.20, CD8 counts: median 662 cells/mL - p = 0.72, r = 0.06; CD4/CD8 ratio: median: 0.58 - p = 0.17, r = -0.24; sCD14: median: 1662 ng/mL - p = 0.26, r = 0.19 – data not shown). *Our data indicate that IL-10 may play a significant role for HIV persistence in ART HIV individuals.*

Significantly higher HIV DNA+ cells in lymph nodes from HIV aviremic individuals are associated with close proximity to IL-10+ cells. We next used several *in situ* quantitative imaging approaches to evaluate the contribution of IL-10 to the cellular and anatomical localization of the HIV reservoir in lymph nodes (LNs). In LNs from HIV negative HC (left plots, n=7) and HIV-aviremics (right plots, n=13), *in situ* immuno-histochemistry (**Fig 1c**) revealed that the frequencies of IL-10+ cells per anatomical area, *i.e* the Follicle (F), T cell zone (TZ) and medullary cord (MC) were significantly increased in HIV aviremic individuals when compared to HC (F: *HIV aviremics: 0.27% IL-10+ cells, FC HIV/HC: 9, p<0.0001*, *TZ: HIV aviremics: 0.46% IL-10+ cells, FC HIV/HC: 9.8, p<0.0001; MC: HIV aviremics: 1.6% IL-10+ cells, FC HIV/HC: 6.4, p=0.0003* – **Fig. 1d** – Mann-Whitney unpaired T test). The contribution of the IL-10 pathway engagement in the maintenance of the HIV reservoir in follicular (F) and extra-follicular (EF) areas of LNs was further

evidenced by the proximity of IL-10+ cells to HIV vDNA+ cells, as well as the proportion of vDNA+ cells that expressed phosphorylated STAT3+ (pSTAT3) cells. DNAscope (vDNA: red), followed by pSTAT3 (green), IL-10 (cyan), CD20 (pink) multiplexed immunofluorescence staining was performed. Representative images from 2 donors show the expression of the selected markers in the follicle (top panel – donor 1) and in the extra-follicular area (bottom panel – donor 2) (**Fig 1e**). While the overall frequency of pSTAT3+ cells was on average 11.3% (SEM ±1.8) in all LN compartments [8.8% (SEM ±1.3; F), 10.6% (SEM ±1.7; EF) and 14.5% (SEM ±2.1; MC)], the frequency of HIV vDNA+ cells that were pSTAT3+ was on average 30.1% (SEM ±5.1) in the LNs of HIV aviremic individuals (n=18) (average quantification from all images as in **Fig 1e** for all donors evaluated). *Importantly, the frequencies of HIV vDNA+ cells increased significantly with their proximity to IL-10+ cells* (0-15uM Median: 60% HIV vDNA+, 15-25uM Median: 25% HIV vDNA+, 35uM Median: 13% HIV vDNA+ cells; 0-15um vs 15-25uM $p>0.05$; 15-25uM vs 35uM $p<0.05$, 0-15um vs 35uM $p<0.01$ – **Fig 1f**) as measured by HALO (Spatial Analysis plot - detailed in methodology). Importantly, 92.6% of all HIV vDNA+ cells were within an average distance of ~3-5 cell diameters (35um) from an IL-10+ cell (quantification from **Fig 1e -** n=18 donors). Our results capture a static snapshot of the LN structure; hence these findings most likely represent an underestimation of the number of infected or IL-10+ cells, as cells in lymph nodes are in constant movement(Huang et al., 2004, Bajenoff et al., 2007, Germain et al., 2012). *Nevertheless, these data strongly and significantly infer the importance of IL-10 signaling in HIV persistence in LNs.*

Several lymphoid and non-lymphoid cell subsets contribute to IL-10 production in LNs of treated chronic aviremic HIV-infected individuals. Using multiparametric confocal imaging and histo-cytometry(Gerner et al., 2012) we demonstrate that several cell subsets including monocytes and macrophages **(Fig S2a** and **Fig 2a)** as well as CD4 T cell subsets and B cells (**Fig S2b** and **Fig 2b)** contributed to IL-10 production in the F and EF areas of LNs. A representative position map is shown in **Fig 2c.** The EF zone presented higher frequencies of IL-10hi cells than F zone (Images in **Fig 2a-b** – IL-10 red dots, quantification in **Fig 2d**- $p<0.05$, FC EF/F: 4.05, n=5). Considering the relative frequencies of IL10hi cells in the F and EF areas in our cohort, IL-10 expressing cells included CD163+/CD68, CD163-/CD68+ and CD163+/CD68+ monocyte/macrophage; the latter cell subset contributed to significant higher frequencies of IL-10 + cells in the EF area than in Follicles (*$p<0.0001$, 1.74-FC increase into EF compared to follicular area*- **Fig 2a and e, n=5**, gating strategy **Fig S2a).** Although most of IL-10+CD4 T cells were FoxP3-, a readily fraction was found to be FoxP3+ in the F and EF areas (*Foxp3+: FC EF/F: 5.72, $p=0.59$; Foxp3-: FC EF/F: 1.37, $p= 0.45$* (**Fig 2b, e,** n=4, gating strategy **Fig S2b)**. In the B cell follicle (BCF), regular immunohistochemistry (IHC) multiplexing markers for B cells (CD20: blue), CD4 cells (red), PD-1 (orange) and IL-10 (green), we observed that Tfh cells (CD4+ PD1+(white circles, **Fig 2f**), contributed to 42% of the IL10+ cells in the BCF (**Fig 1g,** n=11). *Thus, several LN cell subsets can contribute to IL-10 production and could impact on HIV reservoir persistence in this relevant compartment in vivo.*

Pathways associated with cell survival, T cell memory maintenance, co-inhibitory receptors expression, metabolism and Tfh cell differentiation are positively associated with pIL-10 levels and HIV IntDNA. Transcriptional profiling was used to identify the mechanisms downstream of IL-10 that underlie its association with HIV persistence. Gene expression profiles of whole blood from HIV-aviremic individuals were correlated by linear regression analysis with the frequencies of cells harboring HIV IntDNA and to pIL-10 levels (**Fig 3a,** n=22). Gene Set Enrichment Analysis (GSEA)(Subramanian et al., 2005) showed that pathways downstream of IL-10/STAT3 signaling were positively correlated to pIL-10 (NES: 2.16, FDR<10-6, p<10-6) and HIV IntDNA levels (NES1.79, FDR<10-6, p<10-6) (**Fig 3b;** Leading edge genes - LEGs, **Fig S3a)**. Additionally, correlated pathways and genes encoded for molecules with anti-apoptotic properties which are all targets of the JAK-STAT signaling pathway (BIRC5 FYN, BCL2L1, NOTCH, MYC; pIL-10 NES: 1.9, FDR<10-6, p<10-6; HIV IntDNA NES: 1.88, FDR<10-6, p<10-6), as well genes endowed with antiapoptotic functions (BCL2L1, PIM1) or that act as regulators of cell metabolism (MYC, JUN)(Wang et al., 2011) , genes related to glycolysis and glucose catabolic process (STIP1, ENO1, GAPDH - pIL-10 NES: 2.15, FDR<10-6, p<10-6; HIV IntDNA NES: 1.99, FDR<10-6, p<10-6), genes associated to the maintenance of Central Memory T cells, the long-term reservoir (TCM) (CXCR3, EHD4, TOP2A, TNFRSF4 - pIL-10 NES: 3.44, FDR<10-6, p<10-6; HIV IntDNA NES: 2.37, FDR<10-6, p<10-6), genes encoding for co-inhibitory-receptors (LAG3, TIGIT, PDCD1, CTLA4; pIL-10 NES: 2.04, FDR<10-6,

p<10-6; HIV IntDNA NES: 2.03, FDR<10-6, p<10-6) and their downstream signaling targets (PIM3, CASP3, PRMT1, NFKBIZ, KAT2A), as well as genes that define Tfh differentiation (BCL6, MAF, CXCR5, ICOS-ICOSL pIL-10 NES: 1.7, FDR<10-6, p<10-6; HIV IntDNA NES: 1.39, FDR= 0.005, p<10-6) (**Fig 3b –** pathways; and **Fig S3a** – LEGs) were all associated to pIL10 and HIV IntDNA levels (**Table S2 -3**). *These results highlight the contribution of several biological processes (cell survival, induction of Co-IR, cell, memory maintenance, metabolism and Tfh differentiation), importantly STAT3/IL-10 signaling, as associated to ex vivo plasma levels of IL-10, as potential drivers of HIV reservoir persistence.*

IL-10 stimulation in vitro triggers the upregulation of the pathways associated with heightened pIL-10 levels and to the magnitude of the HIV reservoir ex vivo. To confirm the specific role of IL-10 in the induction of the aforementioned pathways associated with HIV reservoir persistence *in vivo*, gene array analysis followed by GSEA was performed on *in vitro* IL-10 stimulated CD4+ T cells from healthy donors. IL-10 induced pathways (**Fig 3c**) and LEGs (**Fig 3d) (Table S4)** were the same as the ones significantly correlated to *ex vivo* levels of pIL-10 and HIV IntDNA. They included the IL-10-transcription factor STAT3, its target genes as well as genes downstream of IL-10 signaling pathway (PDCD1, SOCS3, BCL3, MYC, IFITM1, BCL6 ,JUN, SOD2, STAT3) (NES: 2.72, FDR<10-6, p<10-6), genes encoding for survival and anti-apoptotic pathways (PIM1, NOTCH, MYC, BCL2L - NES: 1.99 FDR<10-6, p<10-6), maintenance of T cell

memory (PIK3CA, IL7R, KLRB1, BTG1 - NES: 1.62 FDR= 6x10-4 p= 0.005), PD1 signaling pathway and exhaustion (PDCD1, CTLA-4, CASP3, BTF3, KAT2A), (PRDX4, ELMO1, IRF4) - NES: 1.69 FDR=5 x 10-4, p<10-6), maintenance of cell metabolism (ALDOA, ENO1, PKM2, LDHA, SGK1,GAPDH, PRDX1 - NES: 1.93 FDR=3.3 x 10-4, p<10-6), and Tfh signaling (BATF, BCL6, ICOS, - NES: 2.31 FDR< 10-6, p<10-6). Importantly, we found that 453 out of 644 IL-10 induced genes that correlated with the frequencies of cells with HIV IntDNA were also transcriptionally regulated by STAT3, *which highlights the restrict regulation of these pathways by IL10/STAT3 signaling.* These STAT3 target genes (ref: (http://www.beaconlab.it/ pscan) also covered all the aforementioned pathways listed as associated with pIL-10 and HIV IntDNA *in vivo* (**Fig S3b** and **c**, respectively – NES and FDR indicated in the figure).

Soluble CD14 (sCD14) is increased in HIV infected individuals and is associated with heightened pIL-10 levels and major pathways associated with HIV persistence in vivo. Bacterial translocation occurs early upon HIV infection(Marchetti et al., 2013) as a consequence of the loss of Th17 cells in the gut(Bixler and Mattapallil, 2013). sCD14 is a validated biomarker for bacterial translocation(Kelesidis et al., 2012) as it is released from activated monocytes upon engagement to lipopolysaccharide (LPS). The engagement of bacterial Pattern recognition receptor (PRRs) to Pathogen-associated molecular pattern (PAMPs) is known to trigger IL-10 production(Yanagawa and Onoe, 2007). Indeed, in our HIV cohort of HIV-aviremics individuals, the plasma levels of sCD14 were

297 significantly increased when compared to HIV negative HCs (HC, n=10, HIV, n=42
298 - FC HIV/HC: 1.20, p<0.05 – **Fig S4a**) and were significantly associated with pIL-
299 10 levels (p=0.007/r=0.53 – **Fig S4b**) indicating that sCD14 could constitute one
300 of the upstream signals leading to heightened pIL-10 levels in these individuals.
301 Supporting this hypothesis, all the pathways associated with heightened pIL-10
302 and HIV reservoir *in vivo*, were also significantly associated with sCD14 levels (IL-
303 10/STAT3 signaling (OASL, IL-10RA, IL4, JAK2 - NES: 2.34, FDR<10-6, p<10-6),
304 survival and anti-apoptosis (TNFR1B, MYD88, GAPD4 -_NES: 2.05, FDR<10-6,
305 p<10-6), maintenance of memory T cells (IL10Ra, TIGIT, TNFRb, SMAD3 -_NES:
306 3.49, FDR<10-6, p<10-6), inhibitory molecules signaling (CTLA4, TIGIT, FYN,
307 BHLHE40 - NES: 2.29, FDR<10-6, p<10-6), maintenance of cell metabolism
308 (ENO1, GAPDH, SLC7A5 -_NES: 2.54, FDR<10-6, p<10-6), and Tfh signaling
309 (CXCR5, CD2, PRDM1 - NES: 1.93 FDR< 10-6, p<10-6)) (Pathways and LEGs -
310 **Fig S4c-d** respectively, **Table S5**). Of note, several transcription factors (TFs)
311 known to bind directly or indirectly to the IL-10 gene promoter(Kubo and Motomura,
312 2012, Zhang and Kuchroo, 2019, Tsuji-Takayama et al., 2008, Cao et al., 2005)
313 including STAT3, BCL-6, MAF, MYC were among the top genes that contributed
314 to the enrichment of these pathways and were significantly associated with sCD14
315 and pIL-10 levels (**Fig S4e**). Overall, 20 pathways were commonly associated with
316 HIV IntDNA, pIL-10, sCD14 and specifically induced by IL-10 stimulation in vitro
317 (**Fig S4f, Table S6**). These pathways included all the aforementioned biological
318 processes (survival, co-IR, cell memory, metabolism and Tfh differentiation).
319 *These data indicate that sCD14 could be one of the mechanisms upstream of IL-*

10 production in HIV-aviremic individuals, contributing to the modulation of pathways associated with HIV persistence.

STAT3 knockout (KO) leads to decreased viral reservoir. To validate experimentally the mechanisms identified by transcriptional profiling associated with HIV persistence and specific to IL-10 signaling we used an *in vitro* model of HIV infection and latency (LARA: Latency and Reversion Assay(Kulpa et al., 2019)) (**Fig S5a**). In this assay, isolated memory CD4+ T cells from healthy individuals are infected *in vitro and* induced to latency by adding TGFb which our group previously established as an inducer of HIV latency *in vitro(Kulpa et al., 2019)*. To confirm the role of IL-10 in the induction of latency, we initially compared it to TGFb. As readout we have evaluated HIV protein expression (p24 – HIV gag) by flow cytometry (**Fig S6a, Table S7**) at different time-points. Addition of IL-10 after *in vitro* infection led to a significantly faster HIV p24 protein expression decay when compared to TGFb [Day 12, Fold Decay (FD) (FD IL-10/TGFb):2.21, $p<0.05$, Day 15, FD1.54, $p<0.05$, Day 17, FD2.85, $p<0.05$ - **Fig 4a***]. Importantly, frequencies of cells with latent HIV provirus, as measured by HIV IntDNA (n=5), were comparable between the two tested conditions (p>0.05 -* ***Fig 4b****), validating IL-10 as an inducer of latency.*

The importance of the IL-10/IL-10Ra-STAT3 axis for the maintenance of HIV (p24) and for the expression of major proteins of each of the pathways associated with HIV IntDNA *ex vivo* that were as well specifically induced by IL-10 *in vitro*, was validated by the blockade of the IL-10 pathway. For this purpose, we either

knocked-out STAT3 by CRISPR-CAS9 editing (STAT3 KO)(Hultquist et al., 2019) or neutralized IL-10 by using an anti-IL-10 monoclonal antibody (mAb)(L., 2005). Addition of anti-IL-10 mAb led to a significant decrease in the phosphorylation of STAT3 even at concentrations as low as 0.1ug/mL ($p<0.05$ - **Fig S5b**). Efficiency of STAT3 knock-out was validated in aCD3/CD28 pre-activated CD4 T cells. The transfection of pre-activated cells led to significant knockout of STAT3 protein detection with all five STAT3 guide RNAs tested (**Fig S5c**). In the LARA model, resting cells are required. Resting memory CD4 T cells were transfected with the combination of two STAT3 guides (guides 3+4) before HIV infection. Non-targeted (NT) guide RNA was used as control. The transfection protocol in resting cells resulted in lower but significant decreased frequencies of STAT3+ cells as measured by flow cytometry (5% full knock-out when compared to the NT guide - $p<0.05$, n=5 – **Fig S5d**). Additionally, STAT3KO induced on average a decay of 27% at per cell level expression of STAT3 (median fluorescence intensity: MFI – range STAT3KO [MFI 349-486]; range NT [MFI 421-695], $p<0.05$ – **Fig S5e**). In line with the gene expression results, STAT3 KO show heightened frequencies of dead cells as a consequence of the removal of survival signals downstream of this transcription factor (**Fig S5f,** $p <0.0001$, Median STAT3hi/dead cells: 34.1%, Median STAT3lo/dead cells: 87.4%) (Left: counter plot gated on STAt3hi x STAt3lo, followed by histogram showing the viability staining in both populations). Knocking out STAT3 prior to infection did not impact the infection rates of these cells with HIV when compared to non-transfected cells or transfected NT (ns: non-significant - **Fig S5g**, n=5). The presence of STAT3hi and STAT3lo cells in resting

366 STAT3-targeted samples allowed us to assess the role of STAT3 in HIV
367 maintenance, and the expression of major proteins of each pathway in the same
368 sample by using a flow-cytometry STAT3 antibody. Gating strategy used for the
369 downstream analysis is shown in **Fig S6 b-d.**
370 STAT3 knockout led to a 10-fold decay in HIV reservoir, quantified by HIV IntDNA
371 per million CD4 T cells, as compared to NT cells after (FC NT/STAT3KO = 3.0,
372 p<0.01 -**Fig 4c** – evaluation performed 14 days after transfection, 11 days after
373 HIV infection and culture in IL-10 supplemented media). Importantly, cultures of
374 NT transfected cells presented similar levels of HIV IntDNA as non-transfected
375 cultures as both experimental conditions were kept in IL-10 containing media as
376 well (p>0.05, **Fig 4c).** T*hese results confirm the role of IL-10 in inducing latency*
377 *and HIV persistence.*
378
379 ***STAT3KO and IL-10 blockade lead to decreased expression of major proteins***
380 ***of key pathways associated with HIV persistence in vivo.*** Next, we used flow
381 cytometry to validate the expression of representative proteins from each of the
382 pathways associated with pIL-10 and HIV reservoir levels *ex vivo* (survival,
383 memory maintenance, Co-inhibitory receptors (Co-IR), metabolism and Tfh cells)
384 in cells from LARA. These experiments were performed after 11 days of culture in
385 IL-10 containing media in transfected and non-transfected cells. The data analysis
386 was performed in an unbiased way using t-distributed stochastic neighbor
387 embedding (TSNE) or Uniform Manifold Approximation and Projection for
388 Dimension Reduction (UMAP). Briefly, a comparable number of events from each

sample was exported and clustered based on the MFI of each marker of interest. Additionally, frequency of cells expressing each marker were quantified. The expression of each marker is provided in both TSNE and UMAP plots (**Fig 4 d** and **g**, respectively) and in heatmaps (**Fig 4 e, f** and **h**). In the STAT3KO-targeted cultures, the STAT3hi cells presented significantly increased expression of BCL2 at per cell level (FC hi/lo: 2.48 – $p<0.001$), increased expression of markers specific to TCM [CCR7 (FC hi/lo: 1.12 – $p=0.06$) and CD27 (FC hi/lo: 1.36 – $p<0.05$)] (**Fig 4e**) and higher TCM / TEM ratios (**Fig S7a –** right counter plot shows TCM x TEM in STAT3hi (red) and STAT3 lo (blue) cells); higher per cell level expression of the Co-IR PD1 (PD1- FC hi/lo: 1.19 – $p<0.05$- **Fig 4e**) and a trend to increased PD1+ cells frequencies (**Fig S7b**) when compared to STAT3lo cells. Importantly, STA3hi cells contributed significantly to the persistence of HIV+ cells (p24- FC hi/lo: 1.26 – $p=0.02$- **Fig 4e**). *STAT3lo cells (BCL2lo CCR7lo CD27lo PD1lo) presented a significant decrease in the expression of p24, supporting the importance of the survival signal, along with the maintenance of the TCM status and the expression of Co-IRs for HIV persistence.*

We used an independent approach (neutralizing anti-IL-10 mAb) to verify the impact of IL-10 on the modulation of the expression of the key proteins measured above. Non-transfected CD4 T cells were infected and treated with IL-10 [10ng/mL] with or without anti-IL-10 [10ug/ml] for 11 days; expression of BCL2, memory markers, PD1 and HIV protein was measured by flow cytometry. The potential of the anti-IL-10 mAb in blocking IL-10 signaling was shown (**Fig S5b**). A significant decrease in BCL2 expression at per cell level was observed in cell cultures treated

with aIL-10, while control cell cultures that received only IL-10 showed increases in BLC2 expression (FC IL-10/aIL-10 1.50, p<0.05 – **Fig 4f**), confirming the transcriptional profiling results (**Fig 3 b-c)**. Addition of IL-10 to cell cultures led to an increase in the expression of markers of TCM cells [CCR7 (FC IL-10/aIL-10: 1.99 – p=0.08) and CD27 (IL-10/aIL-10: 2.03 – p=0.004) - **Fig 4f**], as well as an increase in the frequencies of this subset when compared to TEM cells (**Fig S7c**). The per cell expression levels of PD1 were also significantly increased by IL-10 (FC IL-10/aIL-10 1.61 p<0.05 – **Fig 4f**) as well as its frequencies (FC IL-10/aIL-10: 3.54, p<0.01 **– Fig S7d**). Addition of anti-IL-10 decreased the frequencies of PD1+ cells to levels similar to unstimulated cells. Interestingly, our results are also consistent with published results in cancer pre-clinical models(Turnis et al., 2015, Sawant et al., 2019), where IL-10 levels were associated with heightened Co-IR expression. These results validate at protein levels the gene expression profiling (**Fig 3 b-c)** observed ex vivo and specifically induced by IL-10 *in vitro*.

We next monitored the impact of IL-10 signaling on cell metabolism and HIV persistence as suggested by the transcriptional profiling results. IL-10Ra+ cells presented significantly higher levels of glycolysis as monitored by the higher expression of the glucose importer (Glut-1) (FC IL-10Rp/IL-10Rn: 7.00, p<0.0001 - **Fig 4g-h, Fig S6d**) additional to higher frequencies of cells expressing Glut-1 (FC IL-10Rp/IL-10Rn 2.79, p<0.05 – **FigS7e**). These Glut-1+ cells were significantly enriched in expression of the HIV-envelope (Env) when compared to cells lacking the engagement to the IL-10 pathway (IL-10Ralo cells) (Env MFI FC IL-10Rp/IL-10Rn: 1.25, p=0.02 - **Fig 4g-h**). *Collectively, these results validate the ability of IL-*

10 to regulate the expression of key proteins of the major pathways associated with HIV persistence in vivo. STAT3 KO or neutralization of IL-10 led to decreased expression of the survival protein BCL2, differentiation towards TEM accompanied by downmodulation of PD-1 and decay of immune metabolism resulting in decreased HIV+ cells.

IL-10 leads to Tfh differentiation, a major HIV reservoir compartment. Tfh cells are postulated to be the HIV sanctuary in lymph nodes(Fukazawa et al., 2015, Aid et al., 2018). Accordingly, a gene expression signature specific to Tfh cells were found as positive correlate of HIV reservoir in our human cohort and were specifically induced by IL-10 stimulation *in vitro* (**Fig. 3b-c**, respectively). Target genes common to IL-10/STAT3/Bcl6/c-Maf included the major pathways associated with HIV reservoir *in vivo* (survival, Co-IR and Tfh – **Fig 5a**). Of note, 24 hours stimulation of purified CD4 T cells from healthy donors with IL-10, triggered the expression of surface markers and transcription factors known to be features of Tfh cells (CXCR5, PD1, BCL6 and c-MAF)(Crotty, 2014) (FC IL-10/NS: 3.69, p<0.001- **Fig 5b** - Gating strategy **Fig S8a-c).** Addition of anti-IL-10 abrogated the IL-10 induced upregulation of these markers to similar levels of those of unstimulated cells. Interestingly, in another experiment using whole PBMCs and an unbiased UMAP analysis, IL-10 stimulated cells that presented a Tfh profile (STAT3hi, c-Maf hi, BCL6+) were also IL21+ (FC IL-10/aIL-10: 2.07, p<0.01 – **Fig 5c -**including inset). IL21 exerts an autocrine impact on Tfh differentiation and helps the formation of the germinal center reaction by triggering

458 B cell proliferation and differentiation(Silver and Hunter, 2008). Importantly, in
459 LARA (non-transfected conditions), cells expressing BCL6 were significantly
460 preferentially infected when compared to their BCL6- counterpart (FC
461 BCL6+/BCL6-: 159.1, $p<0.05$ - **Fig 5d** – representative counter plot on top show
462 BCL6 vs HIV-p24) mimicking numerous observations showing Tfh as a foyer for
463 HIV persistence(Thacker et al., 2009, Godinho-Santos et al., 2020, Cai et al.,
464 2019). In chronically treated HIV-infected individuals, Tfh cells become a reservoir
465 sanctuary in the BCF (F), being enriched in HIV IntDNA (**Fig 5e).** *These results*
466 *show that IL-10 by inducing Tfh differentiation in BCF could provide an important*
467 *source of targets for HIV infection and viral persistence.*
468

469 **DISCUSSION**

470 Persistent latent infection requires that HIV infected cells endure over time. Herein,
471 we identified (*in vivo*) and validated (*in vitro*) our hypothesis that IL-10 plays critical
472 role for the maintenance of the HIV reservoir. We have demonstrated that IL-10
473 enhances i) cell survival, ii) upregulates the expression of the co-inhibitory receptor
474 PD-1 (several Co-IRs are part of the gene signature, such as Lag3, TIGIT, CTLA4),
475 which have been previously shown to be involved in the establishment of HIV
476 latency and immune dysfunction(Trautmann et al., 2006, Tzeng et al., 2012, Peng
477 et al., 2008); iii) prevents the differentiation of quiescent TCM to the TEM subset,
478 which we have shown earlier to favor HIV replication(Wonderlich et al., 2019); iv)
479 triggers a *bona fide* metabolic status associated with long lasting cells; and finally,
480 v) we have shown that IL-10 is a potent regulator of Tfh differentiation. *The role of*
481 *IL-10 in HIV persistence is supported by our findings where knocking out STAT3,*

the transcription factor downstream of IL-10/IL-10R engagement(Donnelly et al., 1999), led to decreased frequencies of cells with HIV DNA as a consequence of the downregulation of the key pathways sustaining reservoir survival, latency and longevity (metabolically active TCM cells). We have shown that IL-10 is produced by several cellular subsets including innate immune cells, B cells and T cells i.e most probably Tr1(Zhang and Kuchroo, 2019) or Tfr cells(Laidlaw et al., 2017) in all 3 anatomical sites in the lymph nodes. IL-10 expression is controlled by several transcription factors(Kubo and Motomura, 2012, Zhang and Kuchroo, 2019) that can be triggered by TLRs as shown by our results (NFKB1, EOMES, STAT1) and/or by TCR/CD28 engagement (NFKB1, EOMES, STAT1)(Zhang and Kuchroo, 2019). Microbial products can also trigger B cells and innate immune cells to produce IL-10(Boonstra et al., 2006, Saemann et al., 2000, Liu et al., 2014), which in turn, will promote the differentiation of IL-10 producing Tr1 cells(Asseman and Powrie, 1998). Given that we and others have demonstrated that gastrointestinal tract damage and dysfunction, and microbial translocation persists in individuals on long-term ART(Somsouk et al., 2015), there is a continual systemic source of stimulation that could result in high levels of IL-10 driving viral persistence. Further *in vivo* models suggest a role for the gut flora in triggering IL-10 and regulating homeostatic interactions with commensal microorganisms as IL-10 dependent immunopathology is reversed under germ-free conditions(Sellon et al., 1998). While our results do not discriminate between cells that bind IL-10 and cells that produce IL-10 we provide herein statistically significant evidence that the proximity of IL-10+ cells to HIV DNA+ cells in the LN tissues further supports the

505 notion that IL-10 is important for HIV persistence *in vivo* in tissues. The co-
506 localization of pSTAT3+ and vDNA+ cells to IL-10+ cells, and the increased
507 frequencies of vDNA+ cells in the vicinity of IL10+ cells further implicates this
508 cytokine in promoting HIV persistence in lymph nodes. IL-10 induces latency by
509 downregulating the expression of several transcription factors that are involved in
510 promoting HIV transcription including NFK-b, C/EBPb, NFAT, Ets/PU.1(Schiralli
511 Lester and Henderson, 2012), or by promoting the expression of TFs that can
512 repress HIV LTR activity (PRDM-1)(Kaczmarek Michaels et al., 2015). In the
513 periphery, IL-10 also plays a major role in HIV persistence as demonstrated by the
514 fact that IL-10 was unique among all cytokines that signal through STAT3,
515 including IL-6 and IL-21, to be associated with HIV reservoir size. Differences in
516 signaling and transcriptional activity between IL-10 and IL-6 have been previously
517 reported. Expression of SOCS3 upon IL-10R engagement does not lead to IL-10
518 receptor degradation, keeping IL-10 signaling constant(Niemand et al., 2003).
519 IL-10 signaling enhances the survival of different immune and non-immune cell
520 subsets(Zhou et al., 2001, Levy and Brouet, 1994, Todaro et al., 2006, Boyd et al.,
521 2003) including B cells, which are critical for the maintenance of Tfh
522 numbers(Cubas et al., 2013). While many studies associate IL-10 induced cell
523 survival to BCL2 expression, here we show that the increased survival involves the
524 upregulation of several anti-apoptotic molecules (Bcl2, BclX-l, Pim1, BIRC5)
525 downstream of IL-10 signaling. Enhanced survival could have a direct impact on
526 HIV persistence by enhancing the dissemination of infectious HIV virions to
527 bystander cells in sites where antiviral drugs show poor levels of

528 penetrance(Gavegnano et al., 2017). Additional to endorsing cell survival,
529 homeostatic proliferation(Virgilio and Collins, 2020) and/or clonal expansion(Liu et
530 al., 2020) could further contribute to increased size of the HIV reservoir.
531 Importantly, the usage of an FDA-approved BCL2 antagonist, venetoclax, during
532 HIV reactivation, led to cell death and HIV reservoir decay(Cummins et al., 2017),
533 we also observed that IL-10 signaling blockade led to HIV decay.
534 Our data shows that the heightened levels of pIL-10 is associated with increased
535 expression of Co-IRs, including PD-1, which we and others have shown to trigger
536 T cell quiescence and HIV latency(Evans et al., 2018, Porichis and Kaufmann,
537 2012, Fromentin et al., 2019). Early upon infection, cellular activation leads to PD-
538 1 expression as part of the cascade and HIV preferentially replicates in PD-1+ CD4
539 T cells(Vollbrecht et al., 2010). However, the binding of PD-1 and other Co-IRs to
540 its ligands triggers T cell quiescence(Fromentin et al., 2019); additionally, the
541 expression of PD-1 blocks the differentiation of TCM cells to TEM(Trautmann et
542 al., 2006, Breton et al., 2013, Kulpa et al., 2013). This mechanism provides support
543 for the association between IL-10, PD-1 and frequencies of cells with HIV
544 integrated DNA. Interestingly, the expression of Co-IRs was shown to lead to
545 increased IL-10 production(Dong et al., 1999) upon ligand binding. Of note, we
546 have previously shown that PD-1 stimulation can induce production of IL-10 by
547 myeloid cells and suppression of antiviral immunity(Said et al., 2010). IL-10
548 triggers pathways associated with cell quiescence, and further impedes effector
549 cell differentiation by upregulating transcriptional factors (TFs) associated with
550 maintenance of TCM (TCF7, Notch, FOXO1 and Foxp1(Tang et al., 2012)), and

by downregulating TFs critical for effector function (NFAT, NFKb). Furthermore, as mentioned previously, the upregulation of PD-1 by IL-10 is associated with blockade of T cell memory differentiation and their accumulation as TCM(Trautmann et al., 2006, Breton et al., 2013, Kulpa et al., 2013); this would contribute to the increased accumulation of these cells that are the long-lasting HIV reservoir. Heightened pIL-10 levels have been associated with poor effector function and absence of viral clearance in chronic viral infections(Tian et al., 2016) most probably due to the lack of differentiation of TCM to cells endowed with antiviral effector activity. Relevant to this hypothesis, T cells from IL-10-/- mice exhibited a highly activated phenotype, expressed antiviral cytokines and promoted degranulation in response to cognate Ag-encounter *ex vivo* and were oligoclonal suggesting an ongoing immune response(Jones et al., 2010). In addition to preventing the differentiation of TCM to TEM, IL-10 promotes survival of all memory cell subsets including TEM, which was shown to have the highest levels of inducible HIV(Kulpa et al., 2019). In our experimental model, IL-10 blockade *in vitro,* removed the survival signal, additional to promoting T cell activation, by downmodulating Co-IRs, and differentiation towards TEM.

Importantly, IL-10 helps to fuel cell longevity by promoting a balanced immune metabolism. Much is known about the impact of IL-10 on the metabolism of innate immune cells as it promotes oxidative phosphorylation in macrophages(Ip et al., 2017). IL-10 induces mitophagy that eliminates dysfunctional mitochondria characterized by low membrane potential and a high level of reactive oxygen species(Ip et al., 2017). In the absence of IL-10 signaling, macrophages

accumulate damaged mitochondria(Ip et al., 2017). *Herein, we show that IL-10 triggers enhanced cell metabolism by promoting glycolysis.*

The impact of IL-10 on Tfh differentiation is significant, and to the best of our knowledge this is the first time that these findings are reported. Previous results have shown that IL-10 levels are associated with poor development of functionally mature memory Th1 cells while being positively correlated to increased frequencies of Tfh cells during acute LCMV infection(Tian et al., 2016). Tfh cells are known to harbor HIV intact provirus and can be a source of replication competent virus(Perreau et al., 2013) under ART interruption. Tfh cells provide help for the differentiation and maturation survival of GC B cells(Crotty, 2019), that are known to produce IL-10(Burdin et al., 1997). Additionally, in the GC environment, the IL-10 production is boosted by IL-21, produced by Tfh cells, and the phosphorylation of STAT3 further enhances IL-10 production(Banko et al., 2017). A complex network of TFs, including BCL-6, interferon regulatory factor (IRF4), c-Maf, and BATF, promotes Tfh differentiation while inhibiting alternate CD4 T cell differentiation pathways(Aid et al., 2018), all upregulated at gene and/or protein level in our study and associated with the size of the HIV reservoir. Indeed, Tfh cells were demonstrated to be both productively (i.e., $vRNA^{+}$) and latently (i.e., vDNA) infected at higher frequencies(Perreau et al., 2013, Lindqvist et al., 2012) than non-Tfh cells. Tfh cell accumulate in chronic infection(Maceiras et al., 2017) and this could be related to the higher levels of IL-10 in LNs of HIV-aviremic individuals as shown by our results. Tfh cells can be characterized by the expression of PD1, that is also upregulated by IL-10. Additionally, we have

observed BCL2L12 known to promote T cell survival is also included in the Tfh signature. In the current study, we have shown that IL-10+ and vDNA+ cells are colocalized in the GC area, indicating that aside of promoting the differentiation and survival of the Tfh cells, IL-10 is consequently contributing to the survival of the HIV reservoir in this important compartment.

Pre-clinical interventions using anti-IL-10 have been performed in several studies and despite some concerns regarding safety, have led to positive outcomes. The blockade of IL-10 in the LCMV model led to the inhibition of viral persistence and enhanced T-cell functions(Ejrnaes et al., 2006, Brockman et al., 2009). IL-10 blockade, in addition to clear chronic viral infections in animal models, also improved cytotoxic T cell responses in immunization models(Pitt et al., 2012). In HIV infection, IL-10Ra blockade resulted in markedly increased secretion of IFN-g by CD4+ T cells(Saeidi et al., 2018) as well restored the polyfunctionality of HCV specific T cells(Wilson and Brooks, 2011, Rigopoulou et al., 2005). Dual IL-10R/PD1 blockade further enhanced T cell activity, suggesting that IL-10 and PD-1/PD-L1 are functional through distinct pathways to suppress T cell activity during persistent viral infection(Brooks et al., 2008). Of note, pegylated IL-10 has been shown to enhance CD8 T cell function in cancer patients(Naing et al., 2018, Mumm and Oft, 2013) in sharp contrast to several other studies, where IL-10 negatively impact T cell function(Kahan and Zajac, 2019). Our results show that an anti-IL-10 antibody(L., 2005), was effective in down-regulating *in vitro* the expression of proteins which are part of major pathways associated *in vivo* to HIV persistence, leading to HIV decay in vitro. *Altogether our results feature IL-10 blockade as a*

promising and powerful strategy to revert immune-suppression and to impede on HIV reservoir maintenance leading to a HIV cure.

STAR METHODS

EX VIVO

Cohort. HIV-Aviremic individuals (n= 42) and HIV negative healthy controls (n=10) (**Table S1**) signed informed consent approved by the Royal Victoria Hospital and the CRCHUM Hospital Institutional Review Boards. Plasma, Peripheral blood mononuclear cells (PBMCs) and whole blood paxgene tubes were collected. Plasma viral load was evaluated with the Amplicor HIV-1 Monitor Ultrasensitive Method (Roche)(Sun et al., 1998).

Isolation of CD4+ T cells. PBMCs were isolated from blood samples or leukapheresis products by Ficoll Hypaque density gradient centrifugation(Fuss et al., 2009). Total CD4+ T cells were isolated from PBMCs by negative magnetic selection (Stemcell technologies). The purity of enriched CD4+ T cells was generally greater than 95%, as assessed by flow cytometry (data not shown).

Plasma cytokines quantification. Mutiplex ELISA (Mesoscale): U-PLEX assay (Meso Scale MULTI-ARRAY Technology) commercially available by Meso Scale

643 Discovery (MSD) was used for plasma cytokine detection. This technology allows
644 the evaluation of multiplexed biomarkers by using custom made U-PLEX sandwich
645 antibodies with a SULFO-TAG™ conjugated antibody and next generation of
646 electrochemiluminescence (ECL) detection. The assay was performed according
647 to the manufacturer's instructions
648 (https://www.mesoscale.com/en/technical_resources/technical_literature/techncal
649 _notes_search). In summary, 25µL of plasma from each donor was combined with
650 the biotinylated antibody plus the assigned linker and the SULFO-TAG™
651 conjugated detection antibody; in parallel a multi-analyte calibrator standard was
652 prepared by doing 4-fold serial dilutions. Both samples and calibrators were mixed
653 with the Read buffer and loaded in a 10-spot U-PLEX plate, which was read by the
654 MESO QuickPlex SQ 120. The plasma cytokines values (pg/mL) were
655 extrapolated from the standard curve of each specific analyte. Plasma cytokines
656 levels were analyzed to test for differences between HIV-aviremics and Health
657 Controls (HC). Unpaired non-parametric Mann-Whitney T-test was performed.
658 Negative log 10 (-log10) values of the cytokines was plotted against log2 of the
659 fold change (FC) between HIV aviremics and HIV negative healthy controls. Linear
660 regression and Spearman correlation were performed against HIV IntDNA
661 measures. Negative log 10 (-log10) values of HIV IntDNA was plotted against
662 Spearman rho values HIV aviremics.
663
664 **Integrated HIV DNA quantification.** CD4+ T cells isolated from aviremic donors
665 were digested and cell lysates were directly used in a nested Alu PCR to quantify

both integrated HIV DNA and CD3 gene copy numbers, as previously described(Vandergeeten et al., 2014).

Microarray. Gene signature profile was assessed using Illumina Human version 4 beadchips (Illumina) at 58 °C for 20 h. RNA was isolated using the Rneasy micro kit (Qiagen) and the quantity and quality of the RNA were confirmed using a NanoDrop 2000c (Thermo Fisher Scientific) and an Experion Electrophoresis System. Samples (50 ng) were amplified using Illumina TotalPrep RNA amplification kits (Ambion) as per manufacture instructions. The chips were scanned using Illumina's iSCAN and quantified using Genome Studio (Illumina). Raw beadchips intensities were quantile-normalized and log2-transformed.

Multiparameter confocal imaging. Confocal imaging was performed with formalin fixed paraffin embedded (FFPE) lymph node sections prepared at a ~5 µm thickness. Tissue sections were deparaffinized by bathing in xylene and serial ethanol dilutions. Antigen retrieval was performed at 110°C for 15 minutes using Borg Decloaker RTU (Biocare Medical). Tissue sections were then blocked, permeabilized for 1 hour at room temperature and stained with the following primary and conjugated antibodies: anti-CD20 eFluor 615 (clone L26), anti-Ki67 Brilliant Violet 421 (clone B56), anti-CD4 Alexa Fluor 488 (Goat polyclonal IgG, FAB8165G, R&D systems), anti-IL-10 (rabbit polyclonal, ab34843, Abcam) and either anti FoxP3-Alexa Fluor 647 (clone 206D) or anti CD68 (clone KP-1) and CD163- Alexa Fluor 647 (clone EDHu-1) depending on the panel. The nuclear

689 stain Jojo-1 (Life Technologies) was also used to delineate individual cells.
690 Stainings were carried out consecutively with the primary antibodies being added
691 first and incubated overnight at 4° C, followed by staining with the appropriate
692 secondary antibody which –depending on the panel - was either Alexa Fluor 546
693 goat anti-rabbit IgG for IL-10 (ThermoFisher Scientific, A11010) or Alexa Fluor 488
694 goat anti-mouse IgG1 for CD68 (ThermoFisher Scientific, A21121). Conjugated
695 antibody stainings were performed for 2 hours at room temperature, after which
696 sections were stained with JoJo-1 for nucleus identification. Images were acquired
697 at a 512 x 512 pixel density using a 40x objective (NA 1.3) on a Nikon confocal
698 system running NIS-elements AR. Fluorophore spectral spillover was corrected
699 through live spectral un-mixing (NIKON).
700
701 **Histo-cytometry and imaging analysis**. Post-acquisition analysis was performed
702 using the Imaris software (Bitplane, version 8.4). Histo-cytometry was performed
703 as previously described(Gerner et al., 2012, Petrovas et al., 2017). Briefly,
704 dimensional imaging datasets were segmented based on their nuclear staining
705 signal and average voxel intensities for all channels were extrapolated in Imaris
706 after iso-surface generation. Data were then exported to Microsoft Excel,
707 concatenated into a single comma separated values (csv) format and imported into
708 FlowJo version 10 for further analysis. The results of the histocytometry
709 quantification were expressed as average frequencies.
710

Next-generation HIV DNA in situ hybridization and immunofluorescent detection for confocal phenotypic analysis.

The next-generation *in situ* hybridization method DNAscope(Deleage et al., 2016) and multiplex immunofluorescence staining were performed on 5 µm thick sections from FFPE lymph node biopsies from HIV-1 infected, cART suppressed participants from Emory University and Case-Western Reserve University cohorts, along with FFPE ACH-2 HIV-1 positive controls [obtained through the NIH AIDS Reagent Program, Division of AIDS, NIAID, NIH: ACH-2 Cells from Dr. Thomas Folks (cat# 349)](Clouse et al., 1989, Folks et al., 1989) and human HIV-uninfected lymph node negative controls from the OHSU Biolibrary. DNAscope was performed according to Deleage *et al*(Deleage et al., 2016) with some modifications. Briefly, slides were deparaffinized by heating at 60°C for 1 hour, followed by two 5-minute xylene incubation and two 1-minute 100% ethanol incubations. Slides were then kept in double distilled water for 1 hour before heat induced epitope retrieval using the ACD Target Retrieval Buffer and the Biocare NxGen Decloaking Chamber that was set to 110°C for 15 min. After the Decloaking Chamber was cooled to 95°C, the slides were removed from the chamber and cooled at room temperature for a further 15 minutes. Slides were then rinsed twice in double distilled water and tissues were kept wet throughout the rest of the protocol. Protease treatment was omitted to improve antibody epitope preservation and staining. Slides were incubated for 10 minutes at room temperature with 3% Hydrogen peroxide diluted in PBS to inactivate endogenous peroxidases. The HIV-1 Clade B sense probe (ACDbio cat. No. 425531) was added to the tissue for a

14-hour incubation at 40ºC in a HybEz oven. The ACDBio RNAscope 2.5 Brown kit was used to amplify vDNA signal according to manufacturer's recommendations, with the exception that wash steps were performed with 0.5X RNAscope wash buffer. In addition, after Amp 5 and 6, slides were washed with 1X TBS-Tween-20 (0.05% v/v) instead of ACD wash buffer. Viral DNA fluorescence signal was developed using the ThermoFisher Alexa Fluor (AF)647 Tyramide Reagent followed by boiling in ACDBio Target Retrieval buffer for 10 minutes at 95-100°C to inactivate the HRP. Immunofluorescence antibody staining was performed using a rabbit anti-Human IL-10 antibody (Abcam ab-34843), a rabbit anti-pSTAT3 antibody (Cell Signaling 9145) and a mouse anti-CD20 antibody (Dako M0755). The anti-IL-10 antibody was labelled using an HRP-conjugated polymer anti-rabbit secondary antibody (GBI Labs D13-110) and developed with AF568 Tyramide reagent (ThermoFisher), followed stripping of the primary rabbit antibody and inactivation of the HRP by boiling in ACDBio Target Retrieval buffer for 10 minutes at 95-100°C. Subsequent anti-pSTAT3 and anti-CD20 staining were labelled with AF 750 conjugated anti-rabbit and AF488 conjugated anti-mouse secondary antibodies (ThermoFisher) respectively. Tissues were counterstained with DAPI and cover slipped with #1.5 GOLD SEAL cover glass (EMS) using Prolong® Gold reagent (ThermoFisher).

Quantitative image analysis

To quantify the number of vDNA+, IL-10+ and/or pSTAT3+ cells on stained tissues, whole-slide high-resolution fluorescent scans were performed at 20X using the

Zeiss AxioScan Z.1 slide scanner. DAPI, AF488, AF568, Cy5 (For AF647) and Cy7 (For AF750) channels were used to acquire images. The exposure time for image acquisition was between 4 and 150 ms. Multi-spectral images were analyzed using the HALO 2.3 platform (Indica Labs) using the following analysis methods: For HIV-1 vDNA, cells with clear punctate dots were quantified using the module FISH v1.1. Thresholds for spot size and intensity were standardized against the vDNA signal in ACH-2 cells, which has at least one integrated provirus per cell. Total cell count per tissue was also performed using this module. For the quantification of the total number of pSTAT3+ and IL-10+ cells per tissue, the FISH v1.1 module was also used. The Nearest Neighbor and Proximity Analysis were performed with the Spatial Analysis plot function of HALO, using the object data derived from the previous individual analyses discussed above. Manual curation was performed to confirm the accurate quantification of vDNA+ cells and their individual IL-10 and pSTAT3 status.

IN VITRO

Primary CD4+ T Cell Isolation and Culture. Briefly, primary human CD4+ T cells from healthy donors were isolated from donated leukoreduction chambers. Peripheral blood mononuclear cells (PBMCs) were isolated by Ficoll centrifugation using SepMate tubes (STEMCELL, per manufacturer's instructions). Bulk CD4+ T cells were subsequently isolated from PBMCs by magnetic negative selection using an EasySep Human CD4+ T Cell Isolation Kit (STEMCELL, per manufacturer's instructions). Alternately, memory CD4+ T cells were isolated from

PBMCs by magnetic negative selection using an EasySep™ Human Memory CD4+ T Cell Enrichment Kit (STEMCELL, per manufacturer's instructions). Isolated CD4+ T cells were suspended in complete Roswell Park Memorial Institute (RPMI), consisting of RPMI-1640 (Sigma) supplemented with 5mM 4-(2-hydroxyethyl)-1-piperazineethanesulfonic acid (HEPES, Corning), 2mM Glutamine (UCSF Cell Culture Facility), 50µg/mL penicillin/streptomycin (P/S, Corning), 5mM sodium pyruvate (Corning), and 10% fetal bovine serum (FBS, Gibco).

IL-10 stimulation in vitro

Viable frozen primary human PBMCs cells from healthy donors were thawed, counted and rested for 2 hours at 37C, 5% CO2 at a concentration of 2 million PBMCs/mL in vented cap bottles in complete Roswell Park Memorial Institute (RPMI), consisting of RPMI-1640 (Sigma) supplemented with 5mM 4-(2-hydroxyethyl)-1-piperazineethanesulfonic acid (HEPES, Corning), 2mM Glutamine (UCSF Cell Culture Facility), 50µg/mL penicillin/streptomycin (P/S, Corning), 5mM sodium pyruvate (Corning), and 10% fetal bovine serum (FBS, Gibco). Upon resting, 1 million PBMCs were transferred to 48-well plate left unstimulated or were stimulated with IL-10 [10ng/mL] plus or minus anti-IL-10 [10ug/mL] for 24 hours. Brefeldin (1:1000) was added for extra 6 hours in culture (total 30hours). The expression of Tfh markers (CXCR5, PD1, c-Maf and Bcl6 and IL21) were evaluated by flow cytometry.

To evaluate IL-10 signaling through phosphorylation of STAT3 (pSTAT3), different doses of anti-IL-10 was used [0.1-100ug/mL] in addition to IL-10 [10ng/mL]. pSTAT3 MFI was evaluated after 30 minutes of stimulation by flow cytometry.

Microarray for IL-10 induced specific signatures in CD4 T cells. CD4 T cells were isolated from PBMCs from healthy donors (n= 6) were cultured for 12 hours with 10ng/mL of rIL-10 or left unstimulated. Microarray was performed as for the *ex vivo* experiments.

STAT3KO. RNP Production. Detailed protocols for RNP production and primary CD4+ T cell editing have been previously published(Hultquist et al., 2019). Briefly, lyophilized crRNA and tracrRNA (Dharmacon) were suspended at a concentration of 160 µM in 10 mM Tris-HCL (7.4 pH) with 150 mM KCl. 5µL of 160µM crRNA was mixed with 5µL of 160µM tracrRNA and incubated for 30 min at 37°C. The gRNA:tracrRNA complexes were then mixed gently with 10µL of 40µM Cas9 (UC-Berkeley Macrolab) to form Cas9 ribonucleoproteins (RNPs). Five 3.5µL aliquots were frozen in Lo-Bind 96-well V-bottom plates (E&K Scientific) at -80°C until use. **Editing of Resting Memory CD4+ T Cells.** Each reaction consisted of 30x10^6 CD4 T cells, 3.5 µL RNP, 1 µL Alt-R Cas9 Electroporation Enhancer (100 µM, IDT) and 20 µL electroporation buffer. Immediately after isolation, resting memory CD4+ T cells were suspended and counted. RNPs were thawed and allowed to come to room-temperature. One microliter of Alt-R Cas9 Electroporation Enhancer was added to each RNP mixture with gentle mixing. Immediately prior to

825 electroporation, cells were centrifuged at 400xg for 5 minutes, supernatant was
826 removed by aspiration, and the pellet was resuspended in 20 µL of room-
827 temperature P2 electroporation buffer (Lonza) per reaction. Twenty microliters of
828 cell suspension were then gently mixed with each RNP mixture and aliquoted into
829 an electroporation cuvette for nucleofection with the 4D 96-well shuttle unit (Lonza)
830 using pulse code EH-100. Immediately after electroporation, 80 µL of pre-warmed
831 media without IL-2 was added to each well and cells were allowed to rest for at
832 least one hour in a 37°C cell culture incubator. Subsequently cells were moved to
833 vented-bottomed culture bottles pre-filled with warm complete media with IL-2 at
834 40 IU/mL (for a final concentration of 20 IU/mL). Cells were cultured at 37°C / 5%
835 CO_2 in a dark, humidified cell culture incubator for 4 days to allow for gene knock-
836 out and protein clearance, with additional media added on day 2. To check STAT3
837 knock-out efficiency, 50 µL of mixed culture was removed to a centrifuge tube.
838 Cells were staining for total STAT3 monoclonal antibody by flow cytometry. For the
839 LARA experiments a combination of guides 3 and 4 from Dharmacon was used
840 (CM-003544-03-0020, CM-003544-04-0020).
841
842 **LARA (Latency and Reversion assay).** Briefly, on day 0 memory CD4 T cells
843 were isolated. T cells were immediately knocked out for STAT3 or NT and kept in
844 IL-10 [10ng/mL] containing media or non-transfected and cultivated in cRPMI for
845 2-3 days. On Day 4, cells were HIV infected by spinoculcation with the full-length
846 replication competent HIV clone 89.6. Immediately after spinoculation, cells were
847 resuspended in IL-2 [30U/mL] and Saquinavir [5uM]. Infected cells were incubated

for an additional 2-3 days before being introduced into latency culture conditions. For the transfected conditions latency media was composed of antiretroviral cocktail (ARV) of 100 nM efavirenz, 200 nM raltegravir, and 5 μM saquinavir (NIH AIDS Reagent Program; 4624, 11680, and 4658), IL7 [40ng/mL] and IL-10 [10ng/mL]. Non-transfected conditions were cultured in ARV+ IL-7, ARV+ IL-7+IL-10, ARV+ IL-7+IL-10+aIL-10 [10ug/mL] in order to evaluate the role of IL-10 on latency induction. Gold standard latency inducer media was ARV+ IL-7+TGFb1 [20ng/mL] in media composed 50% of H80 supernatant culture(Kulpa et al., 2019). Cells were maintained in this media for 11 days. Half media change was performed every 3-4 days. HIV protein expression decay as the evaluation of other major proteins, of the IL-10 modulated pathways were accessed by flow cytometry. Ten thousand cells were saved at the last day of latency for HIV IntDNA evaluation in the IL-10 containing media conditions.

Cell Preparation and flow cytometry. PBMCs were prepared from whole blood by ficoll-hypaque density sedimentation and cryopreserved in 10% dimethyl sulfoxide and 90% FBS until thawing for phenotypic analysis. Panels to evaluate Survival, Co-IRs, memory subsets, Immune metabolism, Tfh markers and HIV protein expression were performed. Markers were combined in different panels to address the above questions. Antibodies summarized in **Table S7** were used. Flow cytometry data were analyzed to test for differences among the different stim conditions. All antibodies were properly titrated. The cells were all surface stained for 20 minutes in the dark at room temperature, washed, fixed and permeabilized

using the eBioscience™ Foxp3 / Transcription Factor Staining Buffer Set (Cat# 00-5523-00), as per manufacture instructions. Intracellular staining was performed in Perm-Wash provided by the kit for 45 minutes at 4°C. Samples were then washed and re-suspended in staining buffer for acquisition. Samples were acquired on LSRII flow cytometer (Becton Dickinson, San Jose, CA) and ~500,000 live-gated events were collected. Data were analyzed using Flow-Jo software (TreeStar, Ashland, OR). A lymphocyte gate based on FSC-A and SSC-A was defined. Single cells were then selected using FSC-A x FCS-H gate. Live cells were gated and successive gates to define T cell populations of interest. TSNE analysis (t-distributed stochastic neighbor embedding) or UMAP analysis (Uniform Manifold Approximation and Projection for Dimension Reduction) were performed in live single cells for unbiased evaluation of the distribution of the key markers of the major pathways identifies by gene expression *ex vivo* and *in vitro*.

Reagents, antibodies and viruses. IL-10 from Peprotech was used at 10ng/mL; IL-7 from R&D Systems was used at 40ng/mL; TGFb1 from Peprotech was used at 20 ng/mL; anti-IL-10 was produced and characterized by D. Gorman(L., 2005) specifically for this project, dose-response curve was performed evaluating blockage of STAT3 phosphorylation (**Fig S5b**) and 10ug/mL was used for the downstream analysis. Flow antibodies were acquired from BD, Biolegend, MedMab, Beckman Coulter, eBioscience and titrated for best performance in each flow panel (**Table S7**). Viruses were acquired from NIH reagents program (p89.6) and were produced by the virus core facility at CWRU.

894

895 ***IN SILICO***

896 **Microarray Analysis**. Gene array was performed in PBMCs from HIV aviremic
897 individuals. For each gene, a linear regression model with pIL-10 or HIV intDNA
898 measurements in aviremic individuals as an independent variable and gene
899 expression as a dependent variable was fit using the R package LIMMA. Genes
900 that correlated with both outcomes using a Benjamini– Hochberg corrected p value
901 of 0.05 were selected. Gene sets enrichment analysis (GSEA) in ex vivo samples
902 revealed significant and positive correlation of gene signature with IntDNA and pIL-
903 10 levels. Gene signatures were compiled from MSigDB C2 and C7 and other gene
904 sets available in the literature. The LIMMA package was used to fit a linear
905 regression model to each probe (log2 expression) to respectively IntDNA and pIL-
906 10 levels. Genes that correlated to the outcomes were sorted from high to low
907 using their coefficient correlation for each regression and then submitted to GSEA
908 using the pre-Ranked list option. Signatures significantly enriched in these lists
909 with an FDR cut-off of 5% were selected. GSEA normalized enrichment scores
910 were plotted using pheatmap R package. Color gradient from blue to red depicts
911 the normalized enrichment score ranging from decreased (blue) to increased (red).
912 For the *in vitro* IL-10 induced gene signature the LIMMA R package was used to
913 fit linear regression model with the log2 gene expression as dependent variable
914 and the IL-10 stimulated and IL-10 unstimulated CD4 T cells as independent
915 variables in order to identify genes differentially expressed between CD4 T cells
916 stimulated by IL-10 at 12 hours compared to unstimulated CD4 T cells or genes

correlated to plasma IL-10 levels and HIV integrated DNA from ART suppressed (aviremic) samples. A moderated *t* test was used to assess the statistical significance of the association between gene expression and the groups of interest. The p value was adjusted for multiple testing using Benjamini and Hochberg correction method.

To identify pathways enriched in IL-10 stimulated genes at 12 hours and pathways enriched in genes correlated with plasma IL-10 levels and HIV integrated DNA in ART suppressed individuals, we use The GSEA Java desktop program was downloaded from "http://www.broadinstitute.org/gsea/index.jsp[http://www.broadinstitute.org/gsea/index.jsp]" and the default parameters of GSEA preranked option with the following parameters: gene list ranked by their fold; number of permutations: 1000; enrichment statistic: weighted; seed for permutation: time, ignore genesets with less than 10 genes or more than 5000 genes; and the following pathways databases: Molecular Signatures Database (version 5.1) hallmark genesets[46], canonical pathways (module C2.CP), transcription factor targets (module C3.TFT). Specific transcription factors target signatures including STAT3, BCL6 and MAF were extracted from pscan database (http://www.beaconlab.it/ pscan) and the we used a T follicular helper signature as defined in Aid *et al*(Aid et al., 2018).

For pathways enrichment analyses, we applied a 5% cutoff on the false discovery rate (FDR) and a corrected p value of 0.05 on all the differential expression and the regression analyses. Genes network analyses and representation were

939 performed using GeneMania (http://genemania.org) and DyNet Analyzer
940 application under Cytoscape 3.6.0 (https://cytoscape.org).
941
942 **Pathways enrichment analysis.** Gene set enrichment analysis was performed
943 using GSEA and a compiled set of pathways from public data bases including
944 MSigDB version 5.1 (http://software.broadinstitute.org/gsea/msigdb/) and blood
945 cell marker signatures. To test for the enrichment of IL-10 and PD-1 signaling we
946 used in-house signatures (unpublished data). The GSEA Java desktop program
947 was downloaded from the Broad Institute
948 (http://www.broadinstitute.org/gsea/index.jsp) and used with GSEA Pre-Ranked
949 module parameters (number of permutations: 1,000; enrichment statistic:
950 weighted; seed for permutation: 111; 10 ≤ gene set size ≤ 5,000). We used Dynet
951 Analyzer application implemented in Cytoscape version 3.6.0 to generate gene
952 interacting networks to highlight overlapping genes between the different enriched
953 modules.
954
955 **Statistics.** Data sets were tested for a Gaussian distribution using the D'Agostino-
956 Pearson omnibus normality test. Dependent upon the determination of data
957 normality, correlations against plasma IL-10 concentrations were conducted using
958 either a Pearson or nonparametric Spearman analyses. Longitudinal analyses
959 comparing the concentration of plasma IL-10, the %IL-10$^+$ cells in LN by
960 anatomical site, and vDNA$^+$ cells in LN were calculated using either a Mann-
961 Whitney U test or a Wilcoxon matched-pairs signed rank test dependent upon the

962 replicate pairing and Gaussian distribution of the data. Analyses of the *in vitro*
963 stimulations were conducted using a one-way ANOVA with matching and multiple
964 comparisons with a Tukey correction. All statistical tests were two-sided and not
965 adjusted for multiple comparisons. The shorthand representation of statistical
966 significance is as follows: **P* < 0.05; ***P* < 0.01; ****P* < 0.001; *****P* < 0.0001. Data
967 showing statistical outcomes are represented as mean ± SEM. The above
968 statistical analyses were performed using GraphPad Prism 6.0h. A Ridge
969 Regression was performed for analyzing multiple linear regressions that suffer
970 from co-linearity (plasma IL-10 and $\log_{10}$ HIV IntDNA) using P ≤ 0.20 to balance
971 for type I and II errors.
972 All univariate group-differences were analyzed using a non-parametric Wilcoxon-
973 ranked test. Whereas, all univariate correlation analyses were done using a non-
974 parametric Spearman's test. p<0.05 is reported as significant. MonteCarlo
975 simulation approach implemented in the R package (https://cran.r-
976 project.org/web/packages/MonteCarlo), was used to assess the significance of the
977 overlap between *ex vivo* and *in vitro* pathways. Briefly, we simulated 1 million times
978 3 different lists of pathways having with the same length as the ex vivo and the in
979 vitro pathways. Next, we assessed the number of times the overlap between these
980 3 lists is equal or higher than 47 using the MonteCarlo R function.
981
982 **Datasets Availability.**
983 The published article includes all datasets generated or analyzed during this study.
984

Financial Support. This work was supported by the National Institutes of Health (grants UO1 AI 105937 and RO1 AI 110334 and RO1 AI 11444201), the CWRU Center for AIDS Research (grant AI 36219), DARE (U19 AI 096109), CIAR (AI126603, AI124377) and the Fasenmyer Foundation. Rafick-Pierre Sekaly is the Richard J. Fasenmyer Professor of Immunopathogenesis

Potential conflicts of interest.

The authors declare the following conflicts of interest: LM, BH, DG and DH are employed by Merck Sharp & Dohme Corp., a subsidiary of Merck & Co., Inc., Kenilworth, NJ, USA and/or have financial interests in Merck & Co., Inc., Kenilworth, NJ, USA which also provided research support per reagents generation for this study.

Acknowledgements

We are grateful for the patients and clinical team.

Author contributions: SPR and FPD conceptualized and conceived the experimental approaches. SPR, CNC, JH, CD, EM, DK, LL, XX, BT, JT and CS performed experiments in their area of expertise to address the major question. RB, VM, JPG, NK, CP, MP, SGD, JDE and RPS provided samples and supervised the execution of the major techniques on their labs, contributing to data plot and interpretation. LM, BH, DG, DH developed, synthetized and tested anti-IL-10 monoclonal antibody. MA, JPG provided the bioinformatic analysis and data integration. SPR and RPS wrote the manuscript. DHB, VM, CP, SGD, MP, JDE and RPS, contributed to critical review of the manuscript. All authors contributed

to the manuscript development and have critically reviewed and approved the final version.

Declaration of interests

The authors declare no competing interests.

FIGURE LEGENDS

MAIN

Fig 1. ***Significantly increased levels of circulating and lymph-nodes IL-10 in treated HIV infected individuals (aviremic) is associated with the size of latent HIV reservoir (HIV IntDNA).*** **a)** Cytokine array was performed using Meso-Scale platform (MSD). pIL-10 levels were increased in HIV-aviremic individuals (n=24) when compared to HIV negative Healthy controls (HCs, n=4); **b)** pIL10 levels were positively correlated to latent HIV reservoir as measured by HIV IntDNA; **c)** Representative image of IL-10 expression in LNs from 2 HIV negative HCs (left plots) or 2 HIV-ART individuals (right plots). Brown chromogenic IHC – IL-10+ cells –Brown; tissue color: hematoxylin staining; **d)** Quantification of IL-10+ cells (frequency of total area) in different areas of the LN in HIV negative HC (back, n=7) and HIV-aviremics (blue, n=13). F (Follicle), TZ (T cell zone) and MC (medullary cord) are shown. Mann-Whitney unpaired T test was used to compare the frequencies of IL-10+ cells between different zones: F, TZ and MC; **e)** Representative DNAscope (vDNA: red), followed by pSTAT3 (green), IL-10 (cyan),

CD20 (pink) and DAPI (grey) multiplexed immunofluorescence in two HIV-aviremic. For each subject (1 and 2) the top row (magnification of 20x) 4 plots represent: I - Full staining (overlap of all markers), II – Filtered in pSTAT3 and HIV-vDNA, III – HALO spatial plot, IV – Overlay of I and III. Arrows point to vDNA+P-STAT3+ and arrowheads point to vDNA+P-STAT3- cells. Nearest neighbor and Proximity detection of HIV-1 vDNA+ cells to nearby IL-10+ cells was calculated (plot III). The Spatial Proximity Map (III) shows the location of IL-10+ cells (Yellow dots) and HIV-1 vDNA+ cells (Red dots) as detected and assigned by the HALO software. The nearest IL-10+ cell to each HIV-1 vDNA+ cell is indicated by the Proximity Line (gray); **f)** Frequencies of HIV DNA+ cells in the nearest IL10+ cell area is calculated based on spatial proximity map (III). NS: not significant, *p<0.05, **p<0.01. LN: lymph nodes; IHC: Immunohistochemistry; FC: Fold Change. 5-7uM: diameter of a single cell.

***Fig 2. Several lymphoid and non-lymphoid cell subsets contribute to IL-10 production in LNs of treated chronic aviremic HIV-infected individuals: Monocytes, macrophages, CD4 T cells (Tregs, non-Tregs), B cells and Tfh cells are IL10+ in the LNs from HIV-aviremics individuals*. a)** Representative confocal images (40x) of an LN section of a treated aviremic HIV+ individual showing staining for CD20 (blue), Ki67 (yellow), IL-10 (red), CD68 (Cyan), CD163 (green) and the nuclear stain JoJo (upper row and left panel). Zoomed-in details (upper row - middle and right panels) and single-color captions (bottom row - right panel) are from a representative example of CD68/CD163/IL-10 staining that was

used for the quantitation. Zoomed-in areas are presented in succession and each zoom-in corresponds to the region demarcated by the white enclosure. **b)** Representative confocal images (40x) of LN sections of two treated aviremic HIV+ individuals. Overviews on the left depict the total LN area imaged and distribution of CD20 (blue), Ki67 (cyan), CD4 (green) in the tissues screened. Zoomed-in details show the distribution of CD20 and CD4 in overlay with IL-10 (red) and FoxP3 (magenda) at the follicular ($CD20^{hi/dim}$) and extrafollicular (CD20-) junction as denoted by the white dotted lines. Zoomed areas correspond to the red squares shown in each tissue overview; **c)** IL10 location plot; **d)** Pooled histo-cytometry data (n=5) showing the average frequency of $IL\text{-}10^{hi}$ cells in follicular ($CD20^{hi/dim}$: average 26.75%) versus extra-follicular ($CD20^{-}$: 73.25%) areas as assessed by multiparameter confocal imaging (FC EF/F: 3, $p<0.05$); Gating strategy in **Fig S2**; **e)** Contribution of each of the subsets evaluated by confocal/histo-cytometry for the total frequencies of IL10+ cells in the F and EF. CD20+, CD68+ CD168+, CD163+CD68+, total CD4, CD4+Foxp3-, CD4+Foxp3-, co-stained for IL-10 are shown contributing to 100% cells IL10+ in each area; **f)** Representative IHC in BCF from one HIV aviremic individual: CD20 (blue), IL10 (green), CD4 (red) and PD1 (Orange) staining. White and orange circles highlight CD4+PD1+IL10+, CD4+PD1+IL10- cells, respectively; **g)** Frequencies of CD4+PD1+IL10+ Tfh cells (white circles) are shown.

Fig 3. Pathways associated with cell survival, T cell memory maintenance, co-inhibitory receptors expression, metabolism and Tfh cell differentiation

are positively associated with pIL-10 levels and HIV IntDNA and specifically induced by IL-10 stimulation in vitro. Gene array was performed in whole blood from HIV aviremic individuals. **a**) Linear regression model was performed for each gene with pIL-10 or HIV intDNA as an independent variable. Gene expression as a dependent variable was fit using the R package LIMMA. Genes that correlated with both outcomes using a Benjamini– Hochberg corrected p value of 0.05 were selected. The top 100 genes were plot using pheatmap R package. Rows represent genes and columns represent samples. pIL-10 and HIV IntDNA were used as continuous variables and their log 10 transformed values were shown on the top of the heatmap; **b)** Gene sets enrichment analysis (GSEA) in *ex vivo* samples revealed significant and positive correlation of gene signature with HIV IntDNA and pIL-10 levels. Gene signatures were compiled from MSigDB C2 and C7 and other gene sets available in the literature. The LIMMA package was used to fit a linear regression model to each probe (log2 expression) to respectively HIV IntDNA and pIL-10 levels. Genes that correlated to the outcomes were sorted from high to low using their coefficient correlation for each regression and then submitted to GSEA using the pre Ranked list option. Signatures significantly enriched in these lists with an FDR cut-off of 5% were selected. GSEA normalized enrichment scores were plotted using pheatmap R package. Color gradient from blue to red depicts the normalized enrichment score (NES) ranging from decreased (blue) to increased (red); **c)** IL10 stimulation *in vitro* induces the same pathways associated with higher levels of HIV IntDNA and pIL-10 in chronic HIV infected individuals. Gene array was performed in CD4+ T cells isolated from

healthy donors and stimulated for 12 hours with IL-10 or left unstimulated. Gene induced by IL-10 stimulation *in vitro* at 12 hours compared to unstimulated cells were identified using the LIMMA R package and an adjusted p value cut-off of 0.05. GSEA as described above was used to identify which gene sets are enriched in IL-10 stimulated cells. Gene sets NES of pathways significantly induced by IL-10 are shown in the heatmap. Color gradient from blue to red depicts the enrichment score ranging from decreased (blue) to increased (red). For both panels b and c, pathways involved in the same signaling were grouped into modules of STAT3_IL10 signaling, survival, Tfh signaling, inhibitory molecules signaling, memory signatures and metabolism; **d)** Network representation of Leading-edge genes (LEGs) that contributed significantly to the enrichment of pathways induced by IL10 and shown in panel **c**. Dynet application implemented under Cytoscape was used to generate the network. Red diamonds nodes represent modules name. The edge colors connect genes from each module (STAT3/IL10 signaling: black; Inhibitory molecules signaling: dark blue; CD4 memory signatures: light blue; Tfh signaling: indigo blue; mTOR: purple; Survival: green). Rectangles represent the genes upregulated by IL-10. Highlighted as full red rectangles represent important functional gene for each module.

Fig 4. STAT3 knockout (KO) leads to decreased viral reservoir and to decreased expression of major proteins of key pathways associated with HIV persistence in vivo. Memory CD4+ T cells were isolated from HIV negative healthy controls, infected as in **Fig S3a**, and latency was induced at D3 using IL-

10 (5ng/mL) or TGFb1 (20ng/mL) in media containing H80 cell supernatants(Kulpa et al., 2019), ARVs and IL-7 (40ng/mL). **a)** Frequencies of HIV infected cells (CD4-p24+) were evaluated at (day:D) D6, D12, D15 and D17. IL-10 induces HIV protein expression decay at significantly higher levels than TGFb; **b)** HIV IntDNA copies per/million CD4 T cells evaluation at D17 (ns: non-significant); **c)** Copies of HIV IntDNA per million CD4 T cells after latency induction comparing all conditions cultured in media containing IL-10 (10ng/mL) + IL7 (40ng/mL and ARVs): non-transfected, NT and STAT3KO. Paired t test between conditions: **p<0.01, ***p<0.001. **d)** Expression of major proteins of each of the pathways associated *ex vivo* with pIL-10 and HIV IntDNA levels were evaluated by flow cytometry in CD4 T cells from LARA as described in **Fig S3a** (STAT3, BCL2, HIV-p24, PD1, CCR7 and CD27). TSNE analysis was performed in all samples in a total of 3000 cells/sample CD45RA- gated as in **Fig S4b**. TSNE-heatmap for each marker is shown. Low to high levels of protein expression are depicted in the gradient from blue (low) to red (high). **e)** Heatmap summarizing the findings in the STAT3KO transfected condition comparing STAT3hi to STAT3lo. Each row refers to a specific marker and the p values associated to each of them based on paired t. test comparing STAT3lo x STAT3hi. **f)** Heatmap summarizing the findings in the non-transfected condition comparing IL10 and anti-IL10 containing media conditions. Each row refers to a specific marker and the p values associated to each of them based on paired t. test comparing IL10 x anti-IL10. **g)** Expression of metabolic markers along with HIV-envelope expression was assessed in a second flow panel. Same analysis strategy was applied as in **d).** UMAP-heatmaps show the

gradient of expression oh each of the proteins independently. **h)** Heatmap summarizing the findings in the IL10R+ and IL10R- from STAT3KO transfected condition. Each row refers to a specific marker and the p values associated to each of them based on paired t. test comparing IL10R+ and IL10R-. *p<0.05, **p<0.01, ***p<0.0001, ****p<0.0001. Gate on IL10Ra expression was used since no intracellular staining for STAT3 was performed in this panel.

Fig 5. IL-10 leads to Tfh differentiation, a major HIV reservoir compartment.

a) IL10/STAT3/BCL6/c-maf (red node) LEGs (open dots) are shared and are part of the major pathways associated to pIL-10 levels and HIV IntDNA ex vivo (green nodes). Red-full dots, represent important genes for the function of each pathway. Cytoscape was used to generate the gene network. **b)** PBMCs from healthy donors were treated with IL-10 (10 ng/mL) +/- anti-IL10 mAb (10ug/mL) or left unstimulated in complete media for 24 hours. Brefeldin was added for extra 6 hours in culture (total 30hours). The expression of Tfh markers (CXCR5, PD1), its major transcription factors (c-Maf and Bcl6) as well as the production of IL-21 were evaluated by flow cytometry. **c)** After UMAP analysis, Cluster 19 was specifically induced by IL-10. On top, density plots show the modulation of cluster 19 in the different conditions. This cluster is STAT3hi/c-Mafhi, BCL6+ and IL21+ (counter plots shown in **Fig S8c)**. **d)** In the LARA model, 4 days after infection, BCL6+ cells are significantly preferentially infected when compared to its BCL6- counterpart; top: representative dot plot, bottom: quantification of CD4-p24+ cells in BCL6- or BCL6+ T cells; **e)** Immuno-histochemetry in LNs from HIV aviremics individuals.

Follicular (F) and Extrafollicular (EF) are shown (left image: white dotted line). In the follicles, CD4+ T cells (blue) are enriched in HIV reservoir (HIV DNA – red and white arrows). IL10+ cells are shown (green).

REFERENCES

AID, M., DUPUY, F. P., MOYSI, E., MOIR, S., HADDAD, E. K., ESTES, J. D., SEKALY, R. P., PETROVAS, C. & RIBEIRO, S. P. 2018. Follicular CD4 T Helper Cells As a Major HIV Reservoir Compartment: A Molecular Perspective. *Front Immunol,* 9**,** 895.

ASSEMAN, C. & POWRIE, F. 1998. Interleukin 10 is a growth factor for a population of regulatory T cells. *Gut,* 42**,** 157-8.

AVDIC, S., CAO, J. Z., CHEUNG, A. K., ABENDROTH, A. & SLOBEDMAN, B. 2011. Viral interleukin-10 expressed by human cytomegalovirus during the latent phase of infection modulates latently infected myeloid cell differentiation. *J Virol,* 85**,** 7465-71.

BAJENOFF, M., EGEN, J. G., QI, H., HUANG, A. Y., CASTELLINO, F. & GERMAIN, R. N. 2007. Highways, byways and breadcrumbs: directing lymphocyte traffic in the lymph node. *Trends Immunol,* 28**,** 346-52.

BANKO, Z., POZSGAY, J., SZILI, D., TOTH, M., GATI, T., NAGY, G., ROJKOVICH, B. & SARMAY, G. 2017. Induction and Differentiation of IL-10-Producing Regulatory B Cells from Healthy Blood Donors and Rheumatoid Arthritis Patients. *J Immunol,* 198**,** 1512-1520.

BIXLER, S. L. & MATTAPALLIL, J. J. 2013. Loss and dysregulation of Th17 cells during HIV infection. *Clin Dev Immunol,* 2013**,** 852418.

BOONSTRA, A., RAJSBAUM, R., HOLMAN, M., MARQUES, R., ASSELIN-PATUREL, C., PEREIRA, J. P., BATES, E. E., AKIRA, S., VIEIRA, P., LIU, Y. J., TRINCHIERI, G. & O'GARRA, A. 2006. Macrophages and myeloid dendritic cells, but not plasmacytoid dendritic cells, produce IL-10 in response to MyD88- and TRIF-dependent TLR signals, and TLR-independent signals. *J Immunol,* 177**,** 7551-8.

BOYD, Z. S., KRIATCHKO, A., YANG, J., AGARWAL, N., WAX, M. B. & PATIL, R. V. 2003. Interleukin-10 receptor signaling through STAT-3 regulates the apoptosis of retinal ganglion cells in response to stress. *Invest Ophthalmol Vis Sci,* 44**,** 5206-11.

BRETON, G., CHOMONT, N., TAKATA, H., FROMENTIN, R., AHLERS, J., FILALI-MOUHIM, A., RIOU, C., BOULASSEL, M. R., ROUTY, J. P., YASSINE-DIAB, B. & SEKALY, R. P. 2013. Programmed death-1 is a marker for abnormal distribution of naive/memory T cell subsets in HIV-1 infection. *J Immunol,* 191**,** 2194-204.

BROCKMAN, M. A., KWON, D. S., TIGHE, D. P., PAVLIK, D. F., ROSATO, P. C., SELA, J., PORICHIS, F., LE GALL, S., WARING, M. T., MOSS, K., JESSEN, H., PEREYRA, F., KAVANAGH, D. G., WALKER, B. D. & KAUFMANN, D. E. 2009. IL-10 is up-

regulated in multiple cell types during viremic HIV infection and reversibly inhibits virus-specific T cells. *Blood,* 114**,** 346-56.

BROOKS, D. G., HA, S. J., ELSAESSER, H., SHARPE, A. H., FREEMAN, G. J. & OLDSTONE, M. B. 2008. IL-10 and PD-L1 operate through distinct pathways to suppress T-cell activity during persistent viral infection. *Proc Natl Acad Sci U S A,* 105**,** 20428-33.

BURDIN, N., ROUSSET, F. & BANCHEREAU, J. 1997. B-cell-derived IL-10: production and function. *Methods,* 11**,** 98-111.

CACCIARELLI, T. V., MARTINEZ, O. M., GISH, R. G., VILLANUEVA, J. C. & KRAMS, S. M. 1996. Immunoregulatory cytokines in chronic hepatitis C virus infection: pre- and posttreatment with interferon alfa. *Hepatology,* 24**,** 6-9.

CAI, Y., ABDEL-MOHSEN, M., TOMESCU, C., XUE, F., WU, G., HOWELL, B. J., AI, Y., SUN, J., AZZONI, L., LE COZ, C., ROMBERG, N. & MONTANER, L. J. 2019. BCL6 Inhibitor-Mediated Downregulation of Phosphorylated SAMHD1 and T Cell Activation Are Associated with Decreased HIV Infection and Reactivation. *J Virol,* 93.

CAO, S., LIU, J., SONG, L. & MA, X. 2005. The protooncogene c-Maf is an essential transcription factor for IL-10 gene expression in macrophages. *J Immunol,* 174**,** 3484-92.

CHAHROUDI, A., SILVESTRI, G. & LICHTERFELD, M. 2015. T memory stem cells and HIV: a long-term relationship. *Curr HIV/AIDS Rep,* 12**,** 33-40.

CHOMONT, N., EL-FAR, M., ANCUTA, P., TRAUTMANN, L., PROCOPIO, F. A., YASSINE-DIAB, B., BOUCHER, G., BOULASSEL, M. R., GHATTAS, G., BRENCHLEY, J. M., SCHACKER, T. W., HILL, B. J., DOUEK, D. C., ROUTY, J. P., HADDAD, E. K. & SEKALY, R. P. 2009. HIV reservoir size and persistence are driven by T cell survival and homeostatic proliferation. *Nat Med,* 15**,** 893-900.

CLERICI, M., WYNN, T. A., BERZOFSKY, J. A., BLATT, S. P., HENDRIX, C. W., SHER, A., COFFMAN, R. L. & SHEARER, G. M. 1994. Role of interleukin-10 in T helper cell dysfunction in asymptomatic individuals infected with the human immunodeficiency virus. *J Clin Invest,* 93**,** 768-75.

CLOUSE, K. A., POWELL, D., WASHINGTON, I., POLI, G., STREBEL, K., FARRAR, W., BARSTAD, P., KOVACS, J., FAUCI, A. S. & FOLKS, T. M. 1989. Monokine regulation of human immunodeficiency virus-1 expression in a chronically infected human T cell clone. *J Immunol,* 142**,** 431-8.

COUPER, K. N., BLOUNT, D. G. & RILEY, E. M. 2008. IL-10: the master regulator of immunity to infection. *J Immunol,* 180**,** 5771-7.

CROTTY, S. 2014. T follicular helper cell differentiation, function, and roles in disease. *Immunity,* 41**,** 529-42.

CROTTY, S. 2019. T Follicular Helper Cell Biology: A Decade of Discovery and Diseases. *Immunity,* 50**,** 1132-1148.

CUBAS, R. A., MUDD, J. C., SAVOYE, A. L., PERREAU, M., VAN GREVENYNGHE, J., METCALF, T., CONNICK, E., MEDITZ, A., FREEMAN, G. J., ABESADA-TERK, G., JR., JACOBSON, J. M., BROOKS, A. D., CROTTY, S., ESTES, J. D., PANTALEO, G., LEDERMAN, M. M. & HADDAD, E. K. 2013. Inadequate T follicular cell help impairs B cell immunity during HIV infection. *Nat Med,* 19**,** 494-9.

CUMMINS, N. W., SAINSKI-NGUYEN, A. M., NATESAMPILLAI, S., ABOULNASR, F., KAUFMANN, S. & BADLEY, A. D. 2017. Maintenance of the HIV Reservoir Is Antagonized by Selective BCL2 Inhibition. *J Virol,* 91.

DECALF, J., DESDOUITS, M., RODRIGUES, V., GOBERT, F. X., GENTILI, M., MARQUES-LADEIRA, S., CHAMONTIN, C., MOUGEL, M., CUNHA DE ALENCAR, B. & BENAROCH, P. 2017. Sensing of HIV-1 Entry Triggers a Type I Interferon Response in Human Primary Macrophages. *J Virol,* 91.

DELEAGE, C., WIETGREFE, S. W., DEL PRETE, G., MORCOCK, D. R., HAO, X. P., PIATAK, M., JR., BESS, J., ANDERSON, J. L., PERKEY, K. E., REILLY, C., MCCUNE, J. M., HAASE, A. T., LIFSON, J. D., SCHACKER, T. W. & ESTES, J. D. 2016. Defining HIV and SIV Reservoirs in Lymphoid Tissues. *Pathog Immun,* 1**,** 68-106.

DEMOULIN, J. B., UYTTENHOVE, C., VAN ROOST, E., DELESTRE, B., DONCKERS, D., VAN SNICK, J. & RENAULD, J. C. 1996. A single tyrosine of the interleukin-9 (IL-9) receptor is required for STAT activation, antiapoptotic activity, and growth regulation by IL-9. *Mol Cell Biol,* 16**,** 4710-6.

DONG, H., ZHU, G., TAMADA, K. & CHEN, L. 1999. B7-H1, a third member of the B7 family, co-stimulates T-cell proliferation and interleukin-10 secretion. *Nat Med,* 5**,** 1365-9.

DONNELLY, R. P., DICKENSHEETS, H. & FINBLOOM, D. S. 1999. The interleukin-10 signal transduction pathway and regulation of gene expression in mononuclear phagocytes. *J Interferon Cytokine Res,* 19**,** 563-73.

EJRNAES, M., FILIPPI, C. M., MARTINIC, M. M., LING, E. M., TOGHER, L. M., CROTTY, S. & VON HERRATH, M. G. 2006. Resolution of a chronic viral infection after interleukin-10 receptor blockade. *J Exp Med,* 203**,** 2461-72.

ERIKSSON, S., GRAF, E. H., DAHL, V., STRAIN, M. C., YUKL, S. A., LYSENKO, E. S., BOSCH, R. J., LAI, J., CHIOMA, S., EMAD, F., ABDEL-MOHSEN, M., HOH, R., HECHT, F., HUNT, P., SOMSOUK, M., WONG, J., JOHNSTON, R., SILICIANO, R. F., RICHMAN, D. D., O'DOHERTY, U., PALMER, S., DEEKS, S. G. & SILICIANO, J. D. 2013. Comparative analysis of measures of viral reservoirs in HIV-1 eradication studies. *PLoS Pathog,* 9**,** e1003174.

ESTES, J. D., LI, Q., REYNOLDS, M. R., WIETGREFE, S., DUAN, L., SCHACKER, T., PICKER, L. J., WATKINS, D. I., LIFSON, J. D., REILLY, C., CARLIS, J. & HAASE, A. T. 2006. Premature induction of an immunosuppressive regulatory T cell response during acute simian immunodeficiency virus infection. *J Infect Dis,* 193**,** 703-12.

EVANS, V. A., VAN DER SLUIS, R. M., SOLOMON, A., DANTANARAYANA, A., MCNEIL, C., GARSIA, R., PALMER, S., FROMENTIN, R., CHOMONT, N., SEKALY, R. P., CAMERON, P. U. & LEWIN, S. R. 2018. Programmed cell death-1 contributes to the establishment and maintenance of HIV-1 latency. *AIDS,* 32**,** 1491-1497.

FOLKS, T. M., CLOUSE, K. A., JUSTEMENT, J., RABSON, A., DUH, E., KEHRL, J. H. & FAUCI, A. S. 1989. Tumor necrosis factor alpha induces expression of human immunodeficiency virus in a chronically infected T-cell clone. *Proc Natl Acad Sci U S A,* 86**,** 2365-8.

FROMENTIN, R., BAKEMAN, W., LAWANI, M. B., KHOURY, G., HARTOGENSIS, W., DAFONSECA, S., KILLIAN, M., EPLING, L., HOH, R., SINCLAIR, E., HECHT, F. M., BACCHETTI, P., DEEKS, S. G., LEWIN, S. R., SEKALY, R. P. & CHOMONT, N. 2016.

CD4+ T Cells Expressing PD-1, TIGIT and LAG-3 Contribute to HIV Persistence during ART. *PLoS Pathog,* 12**,** e1005761.

FROMENTIN, R., DAFONSECA, S., COSTINIUK, C. T., EL-FAR, M., PROCOPIO, F. A., HECHT, F. M., HOH, R., DEEKS, S. G., HAZUDA, D. J., LEWIN, S. R., ROUTY, J. P., SEKALY, R. P. & CHOMONT, N. 2019. PD-1 blockade potentiates HIV latency reversal ex vivo in CD4(+) T cells from ART-suppressed individuals. *Nat Commun,* 10**,** 814.

FUKAZAWA, Y., LUM, R., OKOYE, A. A., PARK, H., MATSUDA, K., BAE, J. Y., HAGEN, S. I., SHOEMAKER, R., DELEAGE, C., LUCERO, C., MORCOCK, D., SWANSON, T., LEGASSE, A. W., AXTHELM, M. K., HESSELGESSER, J., GELEZIUNAS, R., HIRSCH, V. M., EDLEFSEN, P. T., PIATAK, M., JR., ESTES, J. D., LIFSON, J. D. & PICKER, L. J. 2015. B cell follicle sanctuary permits persistent productive simian immunodeficiency virus infection in elite controllers. *Nat Med,* 21**,** 132-9.

FUSS, I. J., KANOF, M. E., SMITH, P. D. & ZOLA, H. 2009. Isolation of whole mononuclear cells from peripheral blood and cord blood. *Curr Protoc Immunol,* Chapter 7**,** Unit7 1.

GAVEGNANO, C., BREHM, J. H., DUPUY, F. P., TALLA, A., RIBEIRO, S. P., KULPA, D. A., CAMERON, C., SANTOS, S., HURWITZ, S. J., MARCONI, V. C., ROUTY, J. P., SABBAGH, L., SCHINAZI, R. F. & SEKALY, R. P. 2017. Novel mechanisms to inhibit HIV reservoir seeding using Jak inhibitors. *PLoS Pathog,* 13**,** e1006740.

GERMAIN, R. N., ROBEY, E. A. & CAHALAN, M. D. 2012. A decade of imaging cellular motility and interaction dynamics in the immune system. *Science,* 336**,** 1676-81.

GERNER, M. Y., KASTENMULLER, W., IFRIM, I., KABAT, J. & GERMAIN, R. N. 2012. Histo-cytometry: a method for highly multiplex quantitative tissue imaging analysis applied to dendritic cell subset microanatomy in lymph nodes. *Immunity,* 37**,** 364-76.

GODINHO-SANTOS, A., FOXALL, R. B., ANTAO, A. V., TAVARES, B., FERREIRA, T., SERRA-CAETANO, A., MATOSO, P. & SOUSA, A. E. 2020. Follicular Helper T Cells Are Major Human Immunodeficiency Virus-2 Reservoirs and Support Productive Infection. *J Infect Dis,* 221**,** 122-126.

HERBEIN, G. 2018. The Human Cytomegalovirus, from Oncomodulation to Oncogenesis. *Viruses,* 10.

HERTOGHS, N., GEIJTENBEEK, T. B. H. & RIBEIRO, C. M. S. 2017. Interplay between HIV-1 innate sensing and restriction in mucosal dendritic cells: balancing defense and viral transmission. *Curr Opin Virol,* 22**,** 112-119.

HILLMER, E. J., ZHANG, H., LI, H. S. & WATOWICH, S. S. 2016. STAT3 signaling in immunity. *Cytokine Growth Factor Rev,* 31**,** 1-15.

HUANG, A. Y., QI, H. & GERMAIN, R. N. 2004. Illuminating the landscape of in vivo immunity: insights from dynamic in situ imaging of secondary lymphoid tissues. *Immunity,* 21**,** 331-9.

HULTQUIST, J. F., HIATT, J., SCHUMANN, K., MCGREGOR, M. J., ROTH, T. L., HAAS, P., DOUDNA, J. A., MARSON, A. & KROGAN, N. J. 2019. CRISPR-Cas9 genome engineering of primary CD4(+) T cells for the interrogation of HIV-host factor interactions. *Nat Protoc,* 14**,** 1-27.

IP, W. K. E., HOSHI, N., SHOUVAL, D. S., SNAPPER, S. & MEDZHITOV, R. 2017. Anti-inflammatory effect of IL-10 mediated by metabolic reprogramming of macrophages. *Science,* 356**,** 513-519.

JAKOBSEN, M. R., OLAGNIER, D. & HISCOTT, J. 2015. Innate immune sensing of HIV-1 infection. *Curr Opin HIV AIDS,* 10**,** 96-102.

JOCHUM, S., MOOSMANN, A., LANG, S., HAMMERSCHMIDT, W. & ZEIDLER, R. 2012. The EBV immunoevasins vIL-10 and BNLF2a protect newly infected B cells from immune recognition and elimination. *PLoS Pathog,* 8**,** e1002704.

JONES, M., LADELL, K., WYNN, K. K., STACEY, M. A., QUIGLEY, M. F., GOSTICK, E., PRICE, D. A. & HUMPHREYS, I. R. 2010. IL-10 restricts memory T cell inflation during cytomegalovirus infection. *J Immunol,* 185**,** 3583-92.

KACZMAREK MICHAELS, K., NATARAJAN, M., EULER, Z., ALTER, G., VIGLIANTI, G. & HENDERSON, A. J. 2015. Blimp-1, an intrinsic factor that represses HIV-1 proviral transcription in memory CD4+ T cells. *J Immunol,* 194**,** 3267-74.

KAHAN, S. M. & ZAJAC, A. J. 2019. Immune Exhaustion: Past Lessons and New Insights from Lymphocytic Choriomeningitis Virus. *Viruses,* 11.

KELESIDIS, T., KENDALL, M. A., YANG, O. O., HODIS, H. N. & CURRIER, J. S. 2012. Biomarkers of microbial translocation and macrophage activation: association with progression of subclinical atherosclerosis in HIV-1 infection. *J Infect Dis,* 206**,** 1558-67.

KERFOOT, S. M., YAARI, G., PATEL, J. R., JOHNSON, K. L., GONZALEZ, D. G., KLEINSTEIN, S. H. & HABERMAN, A. M. 2011. Germinal center B cell and T follicular helper cell development initiates in the interfollicular zone. *Immunity,* 34**,** 947-60.

KUBO, M. & MOTOMURA, Y. 2012. Transcriptional regulation of the anti-inflammatory cytokine IL-10 in acquired immune cells. *Front Immunol,* 3**,** 275.

KULPA, D. A., BREHM, J. H., FROMENTIN, R., COOPER, A., COOPER, C., AHLERS, J., CHOMONT, N. & SEKALY, R. P. 2013. The immunological synapse: the gateway to the HIV reservoir. *Immunol Rev,* 254**,** 305-25.

KULPA, D. A., TALLA, A., BREHM, J. H., RIBEIRO, S. P., YUAN, S., BEBIN-BLACKWELL, A. G., MILLER, M., BARNARD, R., DEEKS, S. G., HAZUDA, D., CHOMONT, N. & SEKALY, R. P. 2019. Differentiation into an Effector Memory Phenotype Potentiates HIV-1 Latency Reversal in CD4(+) T Cells. *J Virol,* 93.

L., P. 2005. Interleukin-10 Antibodies. *Schering Corporation, World Intellectual Property Organization;,* NA**,** NA.

LAIDLAW, B. J., LU, Y., AMEZQUITA, R. A., WEINSTEIN, J. S., VANDER HEIDEN, J. A., GUPTA, N. T., KLEINSTEIN, S. H., KAECH, S. M. & CRAFT, J. 2017. Interleukin-10 from CD4(+) follicular regulatory T cells promotes the germinal center response. *Sci Immunol,* 2.

LANDAY, A. L., CLERICI, M., HASHEMI, F., KESSLER, H., BERZOFSKY, J. A. & SHEARER, G. M. 1996. In vitro restoration of T cell immune function in human immunodeficiency virus-positive persons: effects of interleukin (IL)-12 and anti-IL-10. *J Infect Dis,* 173**,** 1085-91.

LEE, G. Q. & LICHTERFELD, M. 2016. Diversity of HIV-1 reservoirs in CD4+ T-cell subpopulations. *Curr Opin HIV AIDS,* 11**,** 383-7.

LEVY, Y. & BROUET, J. C. 1994. Interleukin-10 prevents spontaneous death of germinal center B cells by induction of the bcl-2 protein. *J Clin Invest,* 93**,** 424-8.

LINDQVIST, M., VAN LUNZEN, J., SOGHOIAN, D. Z., KUHL, B. D., RANASINGHE, S., KRANIAS, G., FLANDERS, M. D., CUTLER, S., YUDANIN, N., MULLER, M. I., DAVIS, I., FARBER, D., HARTJEN, P., HAAG, F., ALTER, G., SCHULZE ZUR WIESCH, J. & STREECK, H. 2012. Expansion of HIV-specific T follicular helper cells in chronic HIV infection. *J Clin Invest,* 122**,** 3271-80.

LIU, B. S., CAO, Y., HUIZINGA, T. W., HAFLER, D. A. & TOES, R. E. 2014. TLR-mediated STAT3 and ERK activation controls IL-10 secretion by human B cells. *Eur J Immunol,* 44**,** 2121-9.

LIU, R., SIMONETTI, F. R. & HO, Y. C. 2020. The forces driving clonal expansion of the HIV-1 latent reservoir. *Virol J,* 17**,** 4.

MACEIRAS, A. R., ALMEIDA, S. C. P., MARIOTTI-FERRANDIZ, E., CHAARA, W., JEBBAWI, F., SIX, A., HORI, S., KLATZMANN, D., FARO, J. & GRACA, L. 2017. T follicular helper and T follicular regulatory cells have different TCR specificity. *Nat Commun,* 8**,** 15067.

MARCHETTI, G., TINCATI, C. & SILVESTRI, G. 2013. Microbial translocation in the pathogenesis of HIV infection and AIDS. *Clin Microbiol Rev,* 26**,** 2-18.

MCGARY, C. S., DELEAGE, C., HARPER, J., MICCI, L., RIBEIRO, S. P., PAGANINI, S., KURI-CERVANTES, L., BENNE, C., RYAN, E. S., BALDERAS, R., JEAN, S., EASLEY, K., MARCONI, V., SILVESTRI, G., ESTES, J. D., SEKALY, R. P. & PAIARDINI, M. 2017. CTLA-4(+)PD-1(-) Memory CD4(+) T Cells Critically Contribute to Viral Persistence in Antiretroviral Therapy-Suppressed, SIV-Infected Rhesus Macaques. *Immunity,* 47**,** 776-788 e5.

MCMICHAEL, A. J., BORROW, P., TOMARAS, G. D., GOONETILLEKE, N. & HAYNES, B. F. 2010. The immune response during acute HIV-1 infection: clues for vaccine development. *Nat Rev Immunol,* 10**,** 11-23.

MITTAL, S. K. & ROCHE, P. A. 2015. Suppression of antigen presentation by IL-10. *Curr Opin Immunol,* 34**,** 22-7.

MUMM, J. B. & OFT, M. 2013. Pegylated IL-10 induces cancer immunity: the surprising role of IL-10 as a potent inducer of IFN-gamma-mediated CD8(+) T cell cytotoxicity. *Bioessays,* 35**,** 623-31.

MURRAY, A. J., KWON, K. J., FARBER, D. L. & SILICIANO, R. F. 2016. The Latent Reservoir for HIV-1: How Immunologic Memory and Clonal Expansion Contribute to HIV-1 Persistence. *J Immunol,* 197**,** 407-17.

NAING, A., INFANTE, J. R., PAPADOPOULOS, K. P., CHAN, I. H., SHEN, C., RATTI, N. P., ROJO, B., AUTIO, K. A., WONG, D. J., PATEL, M. R., OTT, P. A., FALCHOOK, G. S., PANT, S., HUNG, A., PEKAREK, K. L., WU, V., ADAMOW, M., MCCAULEY, S., MUMM, J. B., WONG, P., VAN VLASSELAER, P., LEVEQUE, J., TANNIR, N. M. & OFT, M. 2018. PEGylated IL-10 (Pegilodecakin) Induces Systemic Immune Activation, CD8(+) T Cell Invigoration and Polyclonal T Cell Expansion in Cancer Patients. *Cancer Cell,* 34**,** 775-791 e3.

NIEMAND, C., NIMMESGERN, A., HAAN, S., FISCHER, P., SCHAPER, F., ROSSAINT, R., HEINRICH, P. C. & MULLER-NEWEN, G. 2003. Activation of STAT3 by IL-6 and

IL-10 in primary human macrophages is differentially modulated by suppressor of cytokine signaling 3. *J Immunol,* 170**,** 3263-72.

PENG, G., LI, S., WU, W., TAN, X., CHEN, Y. & CHEN, Z. 2008. PD-1 upregulation is associated with HBV-specific T cell dysfunction in chronic hepatitis B patients. *Mol Immunol,* 45**,** 963-70.

PERREAU, M., SAVOYE, A. L., DE CRIGNIS, E., CORPATAUX, J. M., CUBAS, R., HADDAD, E. K., DE LEVAL, L., GRAZIOSI, C. & PANTALEO, G. 2013. Follicular helper T cells serve as the major CD4 T cell compartment for HIV-1 infection, replication, and production. *J Exp Med,* 210**,** 143-56.

PERSAUD, D., PIERSON, T., RUFF, C., FINZI, D., CHADWICK, K. R., MARGOLICK, J. B., RUFF, A., HUTTON, N., RAY, S. & SILICIANO, R. F. 2000. A stable latent reservoir for HIV-1 in resting CD4(+) T lymphocytes in infected children. *J Clin Invest,* 105**,** 995-1003.

PETROVAS, C., FERRANDO-MARTINEZ, S., GERNER, M. Y., CASAZZA, J. P., PEGU, A., DELEAGE, C., COOPER, A., HATAYE, J., ANDREWS, S., AMBROZAK, D., DEL RIO ESTRADA, P. M., BORITZ, E., PARIS, R., MOYSI, E., BOSWELL, K. L., RUIZ-MATEOS, E., VAGIOS, I., LEAL, M., ABLANEDO-TERRAZAS, Y., RIVERO, A., GONZALEZ-HERNANDEZ, L. A., MCDERMOTT, A. B., MOIR, S., REYES-TERAN, G., DOCOBO, F., PANTALEO, G., DOUEK, D. C., BETTS, M. R., ESTES, J. D., GERMAIN, R. N., MASCOLA, J. R. & KOUP, R. A. 2017. Follicular CD8 T cells accumulate in HIV infection and can kill infected cells in vitro via bispecific antibodies. *Sci Transl Med,* 9.

PITT, J. M., STAVROPOULOS, E., REDFORD, P. S., BEEBE, A. M., BANCROFT, G. J., YOUNG, D. B. & O'GARRA, A. 2012. Blockade of IL-10 signaling during bacillus Calmette-Guerin vaccination enhances and sustains Th1, Th17, and innate lymphoid IFN-gamma and IL-17 responses and increases protection to Mycobacterium tuberculosis infection. *J Immunol,* 189**,** 4079-87.

PORICHIS, F. & KAUFMANN, D. E. 2012. Role of PD-1 in HIV pathogenesis and as target for therapy. *Curr HIV/AIDS Rep,* 9**,** 81-90.

RIGOPOULOU, E. I., ABBOTT, W. G., HAIGH, P. & NAOUMOV, N. V. 2005. Blocking of interleukin-10 receptor--a novel approach to stimulate T-helper cell type 1 responses to hepatitis C virus. *Clin Immunol,* 117**,** 57-64.

ROJAS, J. M., AVIA, M., MARTIN, V. & SEVILLA, N. 2017. IL-10: A Multifunctional Cytokine in Viral Infections. *J Immunol Res,* 2017**,** 6104054.

SAEIDI, A., ZANDI, K., CHEOK, Y. Y., SAEIDI, H., WONG, W. F., LEE, C. Y. Q., CHEONG, H. C., YONG, Y. K., LARSSON, M. & SHANKAR, E. M. 2018. T-Cell Exhaustion in Chronic Infections: Reversing the State of Exhaustion and Reinvigorating Optimal Protective Immune Responses. *Front Immunol,* 9**,** 2569.

SAEMANN, M. D., BOHMIG, G. A., OSTERREICHER, C. H., BURTSCHER, H., PAROLINI, O., DIAKOS, C., STOCKL, J., HORL, W. H. & ZLABINGER, G. J. 2000. Anti-inflammatory effects of sodium butyrate on human monocytes: potent inhibition of IL-12 and up-regulation of IL-10 production. *FASEB J,* 14**,** 2380-2.

SAID, E. A., DUPUY, F. P., TRAUTMANN, L., ZHANG, Y., SHI, Y., EL-FAR, M., HILL, B. J., NOTO, A., ANCUTA, P., PERETZ, Y., FONSECA, S. G., VAN GREVENYNGHE, J., BOULASSEL, M. R., BRUNEAU, J., SHOUKRY, N. H., ROUTY, J. P., DOUEK, D. C., HADDAD, E. K. & SEKALY, R. P. 2010. Programmed death-1-induced

interleukin-10 production by monocytes impairs CD4+ T cell activation during HIV infection. *Nat Med,* 16**,** 452-9.

SAWANT, D. V., YANO, H., CHIKINA, M., ZHANG, Q., LIAO, M., LIU, C., CALLAHAN, D. J., SUN, Z., SUN, T., TABIB, T., PENNATHUR, A., CORRY, D. B., LUKETICH, J. D., LAFYATIS, R., CHEN, W., POHOLEK, A. C., BRUNO, T. C., WORKMAN, C. J. & VIGNALI, D. A. A. 2019. Adaptive plasticity of IL-10(+) and IL-35(+) Treg cells cooperatively promotes tumor T cell exhaustion. *Nat Immunol,* 20**,** 724-735.

SCHIRALLI LESTER, G. M. & HENDERSON, A. J. 2012. Mechanisms of HIV Transcriptional Regulation and Their Contribution to Latency. *Mol Biol Int,* 2012**,** 614120.

SELLON, R. K., TONKONOGY, S., SCHULTZ, M., DIELEMAN, L. A., GRENTHER, W., BALISH, E., RENNICK, D. M. & SARTOR, R. B. 1998. Resident enteric bacteria are necessary for development of spontaneous colitis and immune system activation in interleukin-10-deficient mice. *Infect Immun,* 66**,** 5224-31.

SHIVE, C. L., JIANG, W., ANTHONY, D. D. & LEDERMAN, M. M. 2015. Soluble CD14 is a nonspecific marker of monocyte activation. *AIDS,* 29**,** 1263-5.

SILVER, J. S. & HUNTER, C. A. 2008. With a little help from their friends: interleukin-21, T cells, and B cells. *Immunity,* 29**,** 7-9.

SLOBEDMAN, B., BARRY, P. A., SPENCER, J. V., AVDIC, S. & ABENDROTH, A. 2009. Virus-encoded homologs of cellular interleukin-10 and their control of host immune function. *J Virol,* 83**,** 9618-29.

SOMSOUK, M., ESTES, J. D., DELEAGE, C., DUNHAM, R. M., ALBRIGHT, R., INADOMI, J. M., MARTIN, J. N., DEEKS, S. G., MCCUNE, J. M. & HUNT, P. W. 2015. Gut epithelial barrier and systemic inflammation during chronic HIV infection. *AIDS,* 29**,** 43-51.

SUBRAMANIAN, A., TAMAYO, P., MOOTHA, V. K., MUKHERJEE, S., EBERT, B. L., GILLETTE, M. A., PAULOVICH, A., POMEROY, S. L., GOLUB, T. R., LANDER, E. S. & MESIROV, J. P. 2005. Gene set enrichment analysis: a knowledge-based approach for interpreting genome-wide expression profiles. *Proc Natl Acad Sci U S A,* 102**,** 15545-50.

SUN, R., KU, J., JAYAKAR, H., KUO, J. C., BRAMBILLA, D., HERMAN, S., ROSENSTRAUS, M. & SPADORO, J. 1998. Ultrasensitive reverse transcription-PCR assay for quantitation of human immunodeficiency virus type 1 RNA in plasma. *J Clin Microbiol,* 36**,** 2964-9.

TANG, B., BECANOVIC, K., DESPLATS, P. A., SPENCER, B., HILL, A. M., CONNOLLY, C., MASLIAH, E., LEAVITT, B. R. & THOMAS, E. A. 2012. Forkhead box protein p1 is a transcriptional repressor of immune signaling in the CNS: implications for transcriptional dysregulation in Huntington disease. *Hum Mol Genet,* 21**,** 3097-111.

TAYLOR, A., AKDIS, M., JOSS, A., AKKOC, T., WENIG, R., COLONNA, M., DAIGLE, I., FLORY, E., BLASER, K. & AKDIS, C. A. 2007. IL-10 inhibits CD28 and ICOS costimulations of T cells via src homology 2 domain-containing protein tyrosine phosphatase 1. *J Allergy Clin Immunol,* 120**,** 76-83.

THACKER, T. C., ZHOU, X., ESTES, J. D., JIANG, Y., KEELE, B. F., ELTON, T. S. & BURTON, G. F. 2009. Follicular dendritic cells and human immunodeficiency virus type 1 transcription in CD4+ T cells. *J Virol,* 83**,** 150-8.

TIAN, Y., MOLLO, S. B., HARRINGTON, L. E. & ZAJAC, A. J. 2016. IL-10 Regulates Memory T Cell Development and the Balance between Th1 and Follicular Th Cell Responses during an Acute Viral Infection. *J Immunol,* 197**,** 1308-21.

TODARO, M., ZERILLI, M., RICCI-VITIANI, L., BINI, M., PEREZ ALEA, M., MARIA FLORENA, A., MICELI, L., CONDORELLI, G., BONVENTRE, S., DI GESU, G., DE MARIA, R. & STASSI, G. 2006. Autocrine production of interleukin-4 and interleukin-10 is required for survival and growth of thyroid cancer cells. *Cancer Res,* 66**,** 1491-9.

TRAUTMANN, L., JANBAZIAN, L., CHOMONT, N., SAID, E. A., GIMMIG, S., BESSETTE, B., BOULASSEL, M. R., DELWART, E., SEPULVEDA, H., BALDERAS, R. S., ROUTY, J. P., HADDAD, E. K. & SEKALY, R. P. 2006. Upregulation of PD-1 expression on HIV-specific CD8+ T cells leads to reversible immune dysfunction. *Nat Med,* 12**,** 1198-202.

TSUJI-TAKAYAMA, K., SUZUKI, M., YAMAMOTO, M., HARASHIMA, A., OKOCHI, A., OTANI, T., INOUE, T., SUGIMOTO, A., TORAYA, T., TAKEUCHI, M., YAMASAKI, F., NAKAMURA, S. & KIBATA, M. 2008. The production of IL-10 by human regulatory T cells is enhanced by IL-2 through a STAT5-responsive intronic enhancer in the IL-10 locus. *J Immunol,* 181**,** 3897-905.

TURNIS, M. E., ANDREWS, L. P. & VIGNALI, D. A. 2015. Inhibitory receptors as targets for cancer immunotherapy. *Eur J Immunol,* 45**,** 1892-905.

TZENG, H. T., TSAI, H. F., LIAO, H. J., LIN, Y. J., CHEN, L., CHEN, P. J. & HSU, P. N. 2012. PD-1 blockage reverses immune dysfunction and hepatitis B viral persistence in a mouse animal model. *PLoS One,* 7**,** e39179.

VANDERGEETEN, C., FROMENTIN, R., MERLINI, E., LAWANI, M. B., DAFONSECA, S., BAKEMAN, W., MCNULTY, A., RAMGOPAL, M., MICHAEL, N., KIM, J. H., ANANWORANICH, J. & CHOMONT, N. 2014. Cross-clade ultrasensitive PCR-based assays to measure HIV persistence in large-cohort studies. *J Virol,* 88**,** 12385-96.

VIRGILIO, M. C. & COLLINS, K. L. 2020. The Impact of Cellular Proliferation on the HIV-1 Reservoir. *Viruses,* 12.

VOLLBRECHT, T., BRACKMANN, H., HENRICH, N., ROELING, J., SEYBOLD, U., BOGNER, J. R., GOEBEL, F. D. & DRAENERT, R. 2010. Impact of changes in antigen level on CD38/PD-1 co-expression on HIV-specific CD8 T cells in chronic, untreated HIV-1 infection. *J Med Virol,* 82**,** 358-70.

WANG, R., DILLON, C. P., SHI, L. Z., MILASTA, S., CARTER, R., FINKELSTEIN, D., MCCORMICK, L. L., FITZGERALD, P., CHI, H., MUNGER, J. & GREEN, D. R. 2011. The transcription factor Myc controls metabolic reprogramming upon T lymphocyte activation. *Immunity,* 35**,** 871-82.

WEBER-NORDT, R. M., HENSCHLER, R., SCHOTT, E., WEHINGER, J., BEHRINGER, D., MERTELSMANN, R. & FINKE, J. 1996. Interleukin-10 increases Bcl-2 expression and survival in primary human CD34+ hematopoietic progenitor cells. *Blood,* 88**,** 2549-58.

WILSON, E. B. & BROOKS, D. G. 2011. The role of IL-10 in regulating immunity to persistent viral infections. *Curr Top Microbiol Immunol,* 350**,** 39-65.

WONDERLICH, E. R., SUBRAMANIAN, K., COX, B., WIEGAND, A., LACKMAN-SMITH, C., BALE, M. J., STONE, M., HOH, R., KEARNEY, M. F., MALDARELLI, F., DEEKS, S. G.,

BUSCH, M. P., PTAK, R. G. & KULPA, D. A. 2019. Effector memory differentiation increases detection of replication-competent HIV-l in resting CD4+ T cells from virally suppressed individuals. *PLoS Pathog,* 15**,** e1008074.

YANAGAWA, Y. & ONOE, K. 2007. Enhanced IL-10 production by TLR4- and TLR2-primed dendritic cells upon TLR restimulation. *J Immunol,* 178**,** 6173-80.

YANG, O. O. 2009. Assessing the antiviral activity of HIV-1-specific cytotoxic T lymphocytes. *Methods Mol Biol,* 485**,** 407-15.

ZEVIN, A. S., MCKINNON, L., BURGENER, A. & KLATT, N. R. 2016. Microbial translocation and microbiome dysbiosis in HIV-associated immune activation. *Curr Opin HIV AIDS,* 11**,** 182-90.

ZHANG, H. & KUCHROO, V. 2019. Epigenetic and transcriptional mechanisms for the regulation of IL-10. *Semin Immunol,* 44**,** 101324.

ZHOU, J. H., BROUSSARD, S. R., STRLE, K., FREUND, G. G., JOHNSON, R. W., DANTZER, R. & KELLEY, K. W. 2001. IL-10 inhibits apoptosis of promyeloid cells by activating insulin receptor substrate-2 and phosphatidylinositol 3'-kinase. *J Immunol,* 167**,** 4436-42.

Fig 1

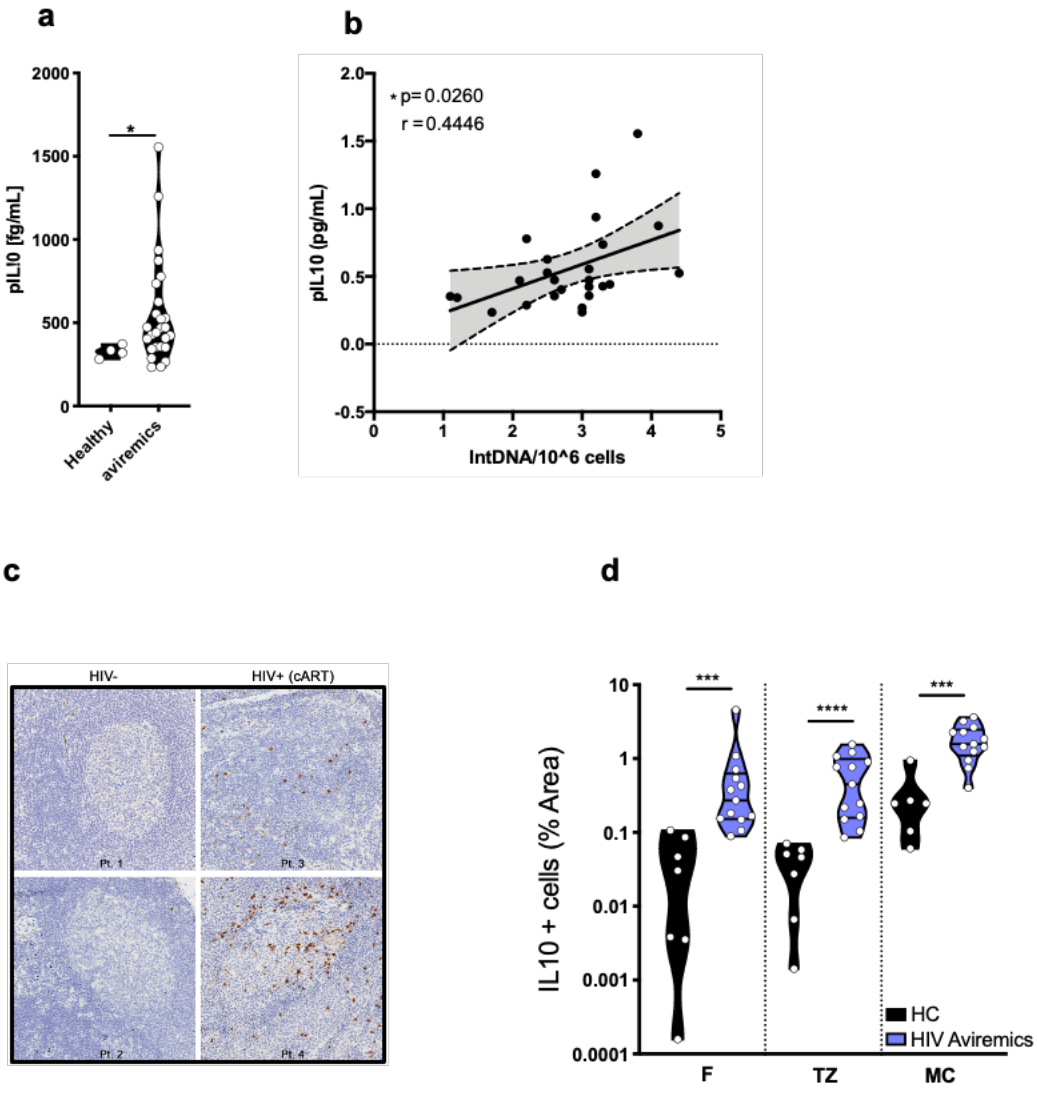
a
b
c
d
pIL10 [fg/mL]
2000
1500
1000
500
0
*
Healthy
aviremics
pIL10 (pg/mL)
* p= 0.0260
r = 0.4446
IntDNA/10^6 cells
HIV-
HIV+ (cART)
Pt. 1
Pt. 3
Pt. 2
Pt. 4
IL10 + cells (% Area)
10
1
0.1
0.01
0.001
0.0001
***
****
***
HC
HIV Aviremics
F
TZ
MC

e

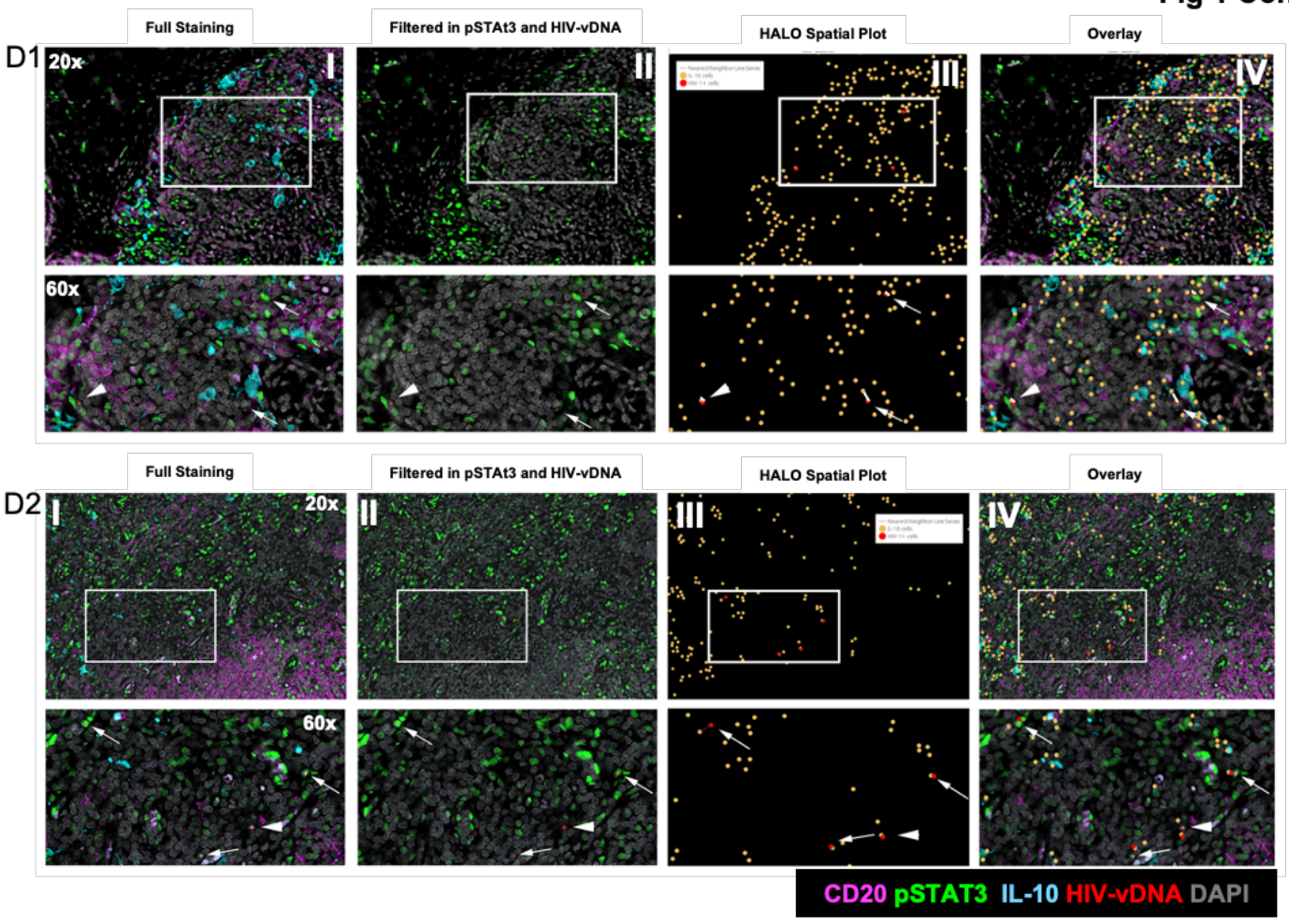
Full Staining
Filtered in pSTAt3 and HIV-vDNA
HALO Spatial Plot
Overlay
D1
20x
60x
I
II
III
IV
D2
CD20 pSTAT3 IL-10 HIV-vDNA DAPI

f

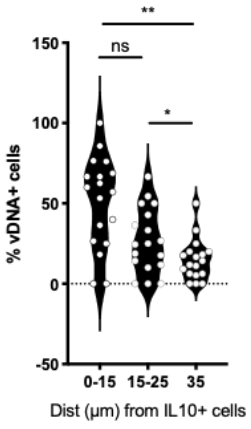
**
ns
*
150
100
50
0
-50
% vDNA+ cells
0-15
15-25
35
Dist (µm) from IL10+ cells

a

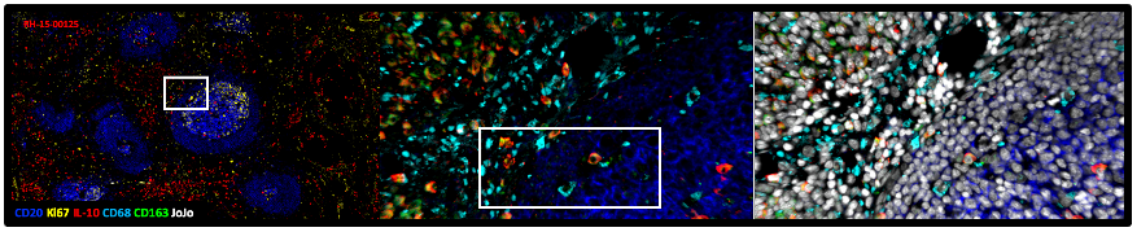
RH-15-00125
CD20 Ki67 IL-10 CD68 CD163 JoJo

b

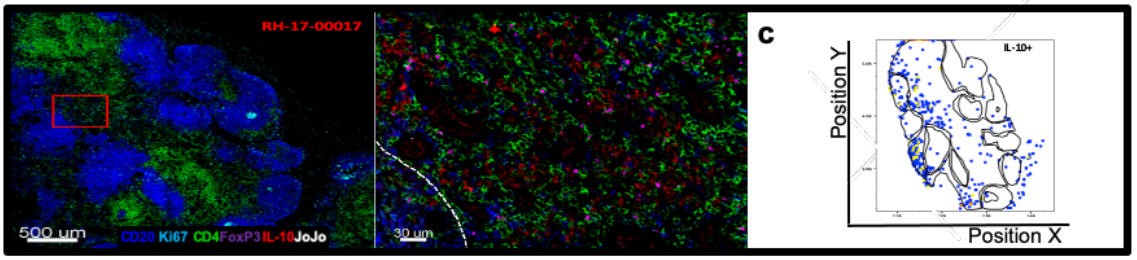
RH-17-00017
500 um
CD20 Ki67 CD4FoxP3IL-10JoJo
30 um

c

IL-10+
Position Y
Position X

d

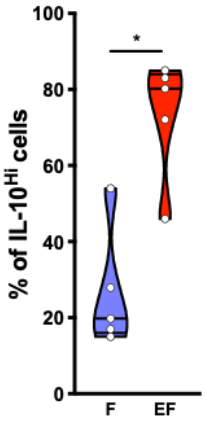
% of IL-10Hi cells
100
80
60
40
20
0
*
F
EF

e

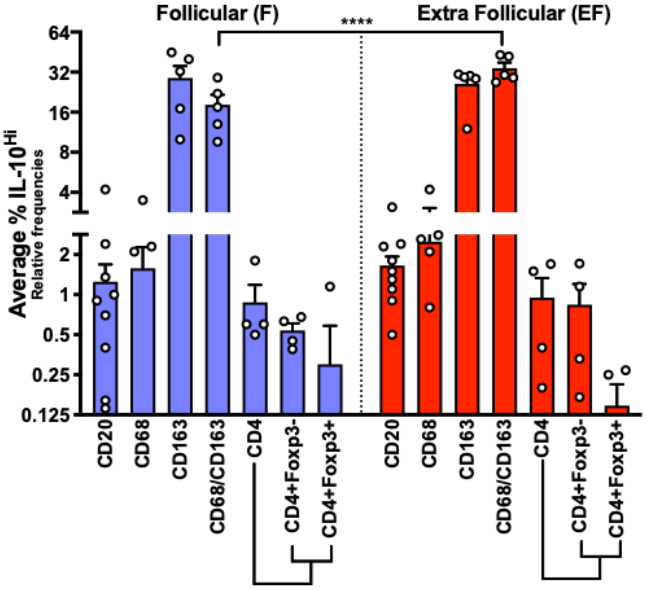
Follicular (F)
****
Extra Follicular (EF)
Average % IL-10Hi
Relative frequencies
64
32
16
8
4
2
1
0.5
0.25
0.125
CD20
CD68
CD163
CD68/CD163
CD4
CD4+Foxp3-
CD4+Foxp3+

f

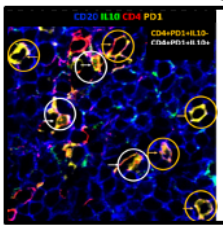
CD20 IL10 CD4 PD1
CD4+PD1+IL10-
CD4+PD1+IL10+

g

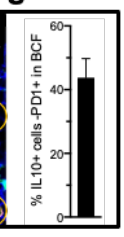
% IL10+ cells -PD1+ in BCF
60
40
20
0

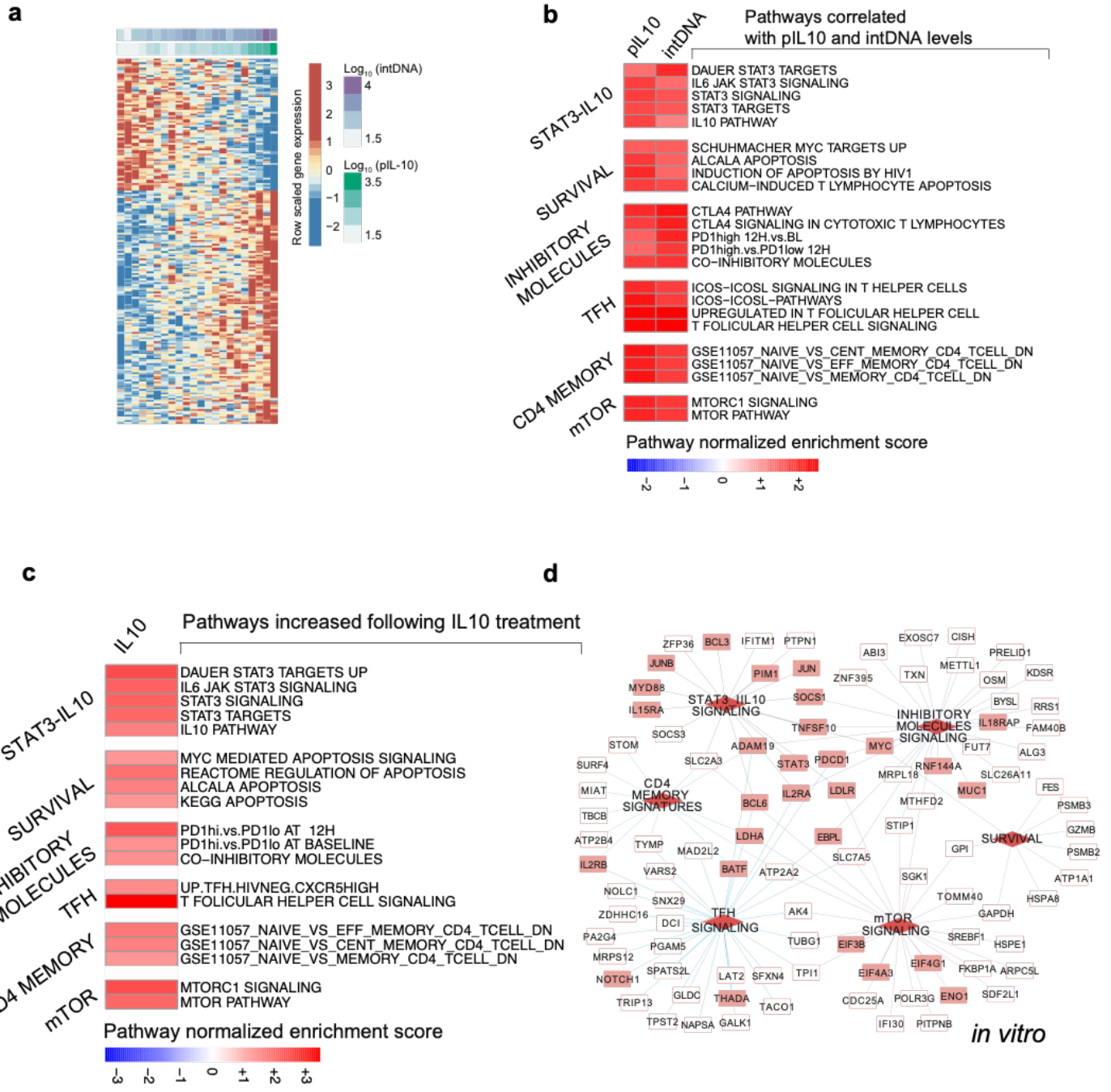
a
Row scaled gene expression
3
2
1
0
−1
−2
Log10 (intDNA)
4
1.5
Log10 (pIL-10)
3.5
1.5
b
pIL10
intDNA
Pathways correlated with pIL10 and intDNA levels
STAT3-IL10
DAUER STAT3 TARGETS
IL6 JAK STAT3 SIGNALING
STAT3 SIGNALING
STAT3 TARGETS
IL10 PATHWAY
SURVIVAL
SCHUHMACHER MYC TARGETS UP
ALCALA APOPTOSIS
INDUCTION OF APOPTOSIS BY HIV1
CALCIUM−INDUCED T LYMPHOCYTE APOPTOSIS
INHIBITORY MOLECULES
CTLA4 PATHWAY
CTLA4 SIGNALING IN CYTOTOXIC T LYMPHOCYTES
PD1high 12H.vs.BL
PD1high.vs.PD1low 12H
CO−INHIBITORY MOLECULES
TFH
ICOS−ICOSL SIGNALING IN T HELPER CELLS
ICOS−ICOSL−PATHWAYS
UPREGULATED IN T FOLICULAR HELPER CELL
T FOLICULAR HELPER CELL SIGNALING
CD4 MEMORY
GSE11057_NAIVE_VS_CENT_MEMORY_CD4_TCELL_DN
GSE11057_NAIVE_VS_EFF_MEMORY_CD4_TCELL_DN
GSE11057_NAIVE_VS_MEMORY_CD4_TCELL_DN
mTOR
MTORC1 SIGNALING
MTOR PATHWAY
Pathway normalized enrichment score
−2
−1
0
+1
+2
c
IL10
Pathways increased following IL10 treatment
STAT3-IL10
DAUER STAT3 TARGETS UP
IL6 JAK STAT3 SIGNALING
STAT3 SIGNALING
STAT3 TARGETS
IL10 PATHWAY
SURVIVAL
MYC MEDIATED APOPTOSIS SIGNALING
REACTOME REGULATION OF APOPTOSIS
ALCALA APOPTOSIS
KEGG APOPTOSIS
INHIBITORY MOLECULES
PD1hi.vs.PD1lo AT 12H
PD1hi.vs.PD1lo AT BASELINE
CO−INHIBITORY MOLECULES
TFH
UP.TFH.HIVNEG.CXCR5HIGH
T FOLICULAR HELPER CELL SIGNALING
CD4 MEMORY
GSE11057_NAIVE_VS_EFF_MEMORY_CD4_TCELL_DN
GSE11057_NAIVE_VS_CENT_MEMORY_CD4_TCELL_DN
GSE11057_NAIVE_VS_MEMORY_CD4_TCELL_DN
mTOR
MTORC1 SIGNALING
MTOR PATHWAY
Pathway normalized enrichment score
−3
−2
−1
0
+1
+2
+3
d
ZFP36
BCL3
IFITM1
PTPN1
JUNB
PIM1
JUN
MYD88
IL15RA
STAT3_IL10 SIGNALING
SOCS1
SOCS3
TNFSF10
STOM
ADAM19
MYC
SURF4
SLC2A3
STAT3
PDCD1
MIAT
CD4 MEMORY SIGNATURES
BCL6
IL2RA
LDLR
TBCB
LDHA
EBPL
ATP2B4
TYMP
MAD2L2
IL2RB
VARS2
BATF
ATP2A2
NOLC1
SNX29
ZDHHC16
DCI
TFH SIGNALING
AK4
PA2G4
PGAM5
TUBG1
MRPS12
SPATS2L
LAT2
SFXN4
TPI1
NOTCH1
TRIP13
GLDC
THADA
TACO1
TPST2
NAPSA
GALK1
ABI3
EXOSC7
CISH
PRELID1
METTL1
ZNF395
TXN
OSM
KDSR
INHIBITORY MOLECULES SIGNALING
BYSL
RRS1
IL18RAP
FAM40B
FUT7
ALG3
RNF144A
MRPL18
SLC26A11
MUC1
FES
MTHFD2
PSMB3
STIP1
GZMB
SURVIVAL
GPI
PSMB2
SLC7A5
SGK1
ATP1A1
TOMM40
HSPA8
GAPDH
mTOR SIGNALING
SREBF1
EIF3B
HSPE1
EIF4G1
FKBP1A
ARPC5L
EIF4A3
CDC25A
POLR3G
ENO1
SDF2L1
IFI30
PITPNB
in vitro

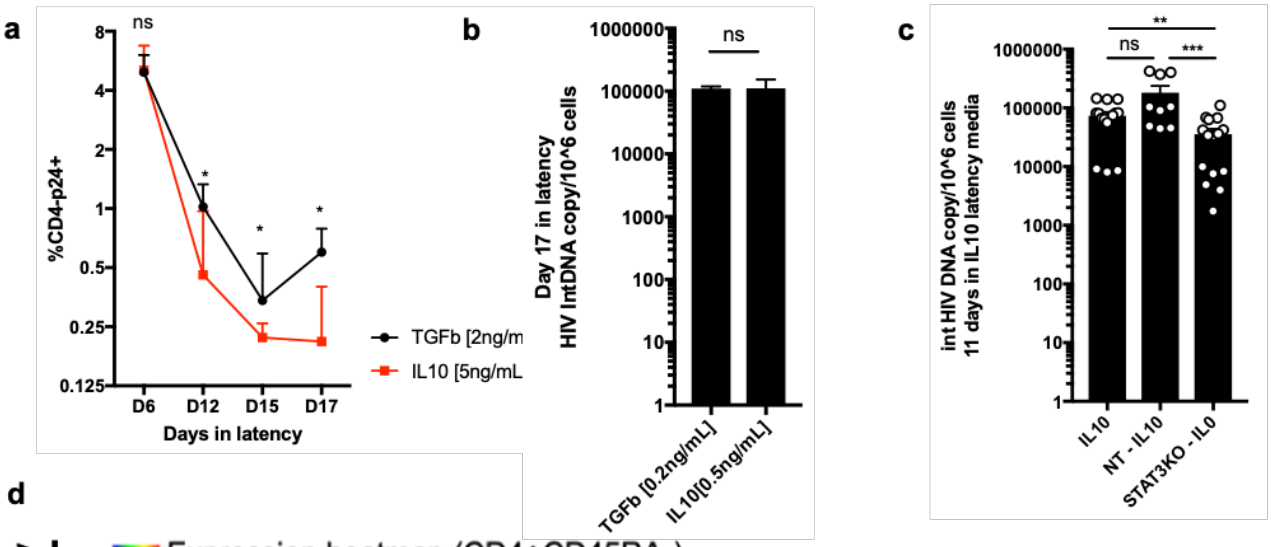
a
ns
%CD4-p24+
Days in latency
D6
D12
D15
D17
TGFb [2ng/m
IL10 [5ng/mL
b
ns
Day 17 in latency
HIV IntDNA copy/10^6 cells
TGFb [0.2ng/mL]
IL10[0.5ng/mL]
c
**
ns
***
int HIV DNA copy/10^6 cells
11 days in IL10 latency media
IL10
NT - IL10
STAT3KO - IL0

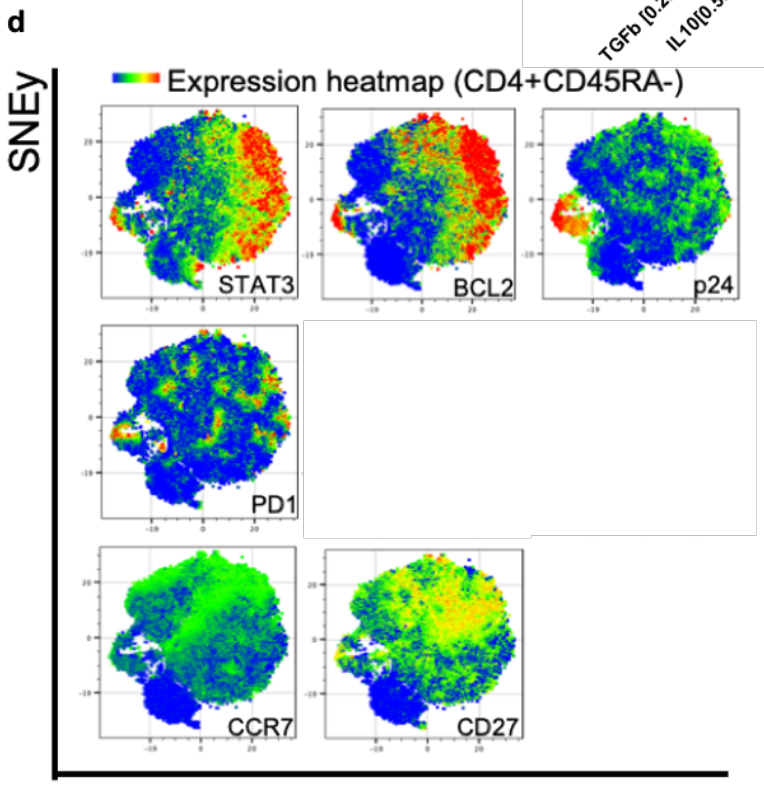
d
Expression heatmap (CD4+CD45RA-)
SNEy
SNEx
STAT3
BCL2
p24
PD1
CCR7
CD27

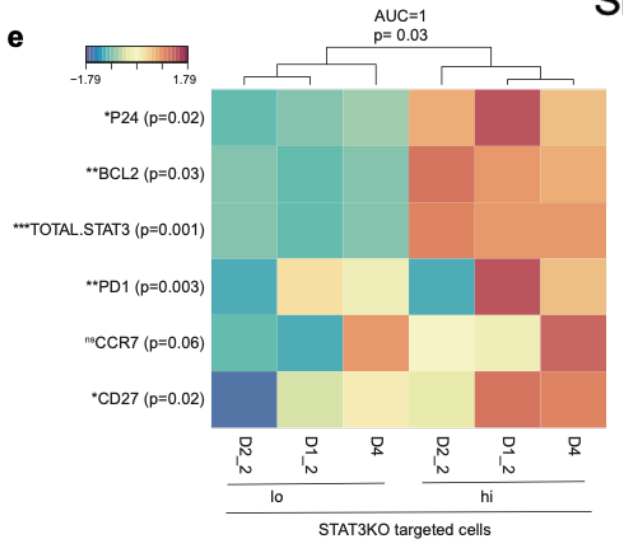
e
AUC=1
p= 0.03
−1.79
1.79
*P24 (p=0.02)
**BCL2 (p=0.03)
***TOTAL.STAT3 (p=0.001)
**PD1 (p=0.003)
ns CCR7 (p=0.06)
*CD27 (p=0.02)
D2_2
D1_2
D4
lo
hi
STAT3KO targeted cells

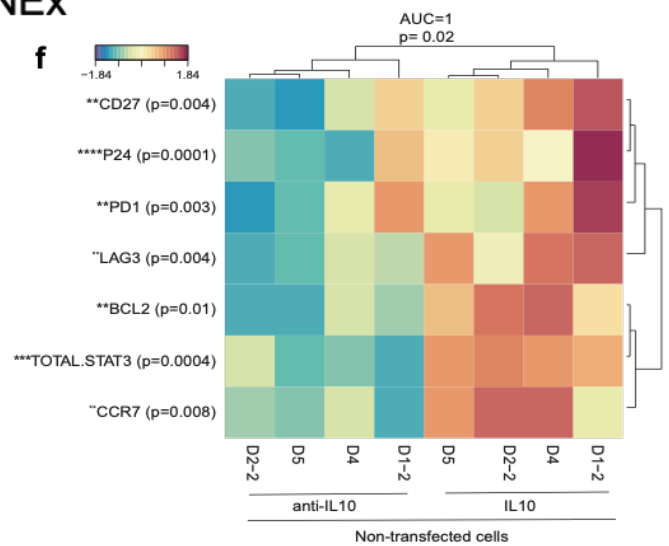
f
AUC=1
p= 0.02
−1.84
1.84
**CD27 (p=0.004)
****P24 (p=0.0001)
**PD1 (p=0.003)
**LAG3 (p=0.004)
**BCL2 (p=0.01)
***TOTAL.STAT3 (p=0.0004)
**CCR7 (p=0.008)
D2~2
D5
D4
D1~2
anti-IL10
IL10
Non-transfected cells

g

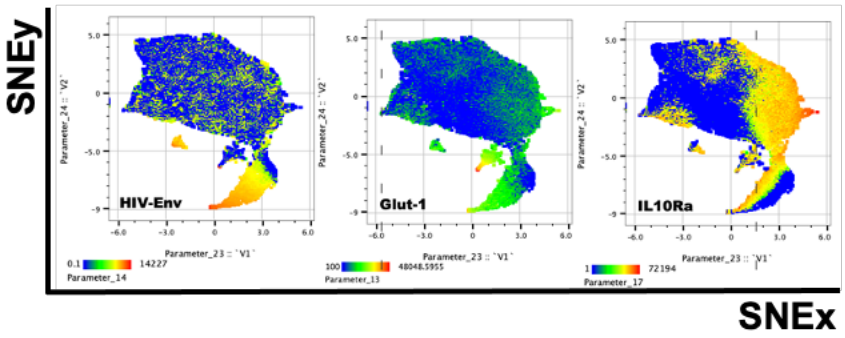
SNEy
HIV-Env
Glut-1
IL10Ra
SNEx

h

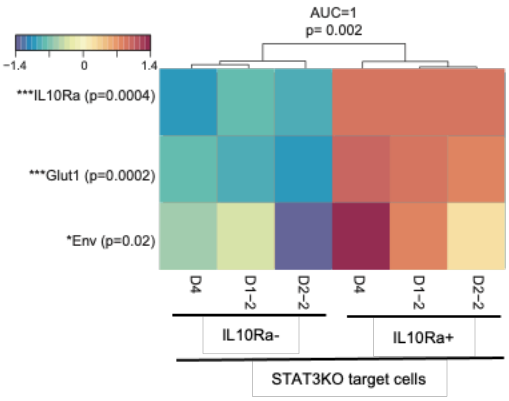
AUC=1
p= 0.002
***IL10Ra (p=0.0004)
***Glut1 (p=0.0002)
*Env (p=0.02)
D4
D1~2
D2~2
IL10Ra-
IL10Ra+
STAT3KO target cells

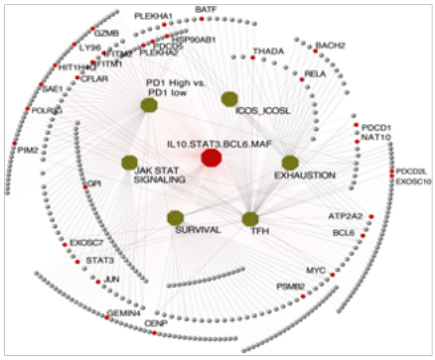
a
PLEKHA1
BATF
GZMB
LY96
HSP90AB1
PDCD1
PLEKHA2
THADA
BACH2
IFITM2
IFITM1
HIT1HA2
CFLAR
RELA
UAE1
PD1 High vs. PD1 low
ICOS_ICOSL
POLR2J
PDCD1
NAT10
PIM2
IL10.STAT3.BCL6.MAF
JAK STAT SIGNALING
EXHAUSTION
PDCD2L
EXOSC10
GPI
ATP2A2
SURVIVAL
TFH
BCL6
EXOSC7
STAT3
MYC
JUN
PSMB2
GEMIN4
CENP

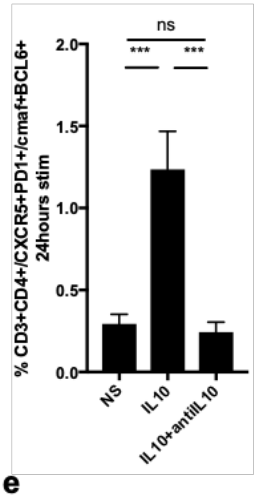
b
% CD3+CD4+/CXCR5+PD1+/cmaf+BCL6+ 24hours stim
ns
***
***
2.0
1.5
1.0
0.5
0.0
NS
IL10
IL10+antiIL10

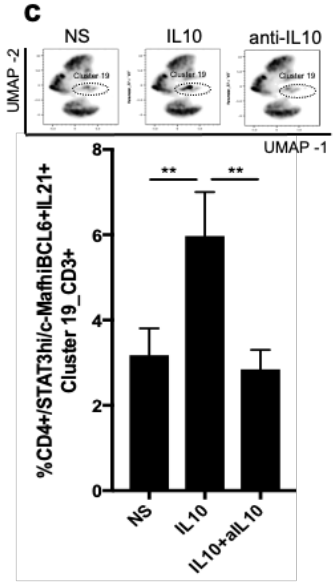
c
NS
IL10
anti-IL10
UMAP -2
UMAP -1
Cluster 19
%CD4+/STAT3hi/c-MafhiBCL6+IL21+ Cluster 19_CD3+
**
**
8
6
4
2
0
NS
IL10
IL10+aIL10

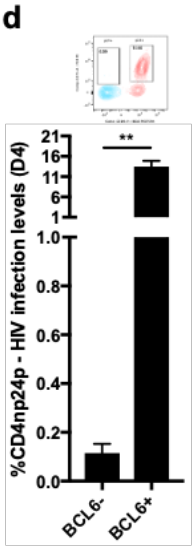
d
%CD4np24p - HIV infection levels (D4)
**
21
16
11
6
1
1.0
0.8
0.6
0.4
0.2
0.0
BCL6-
BCL6+

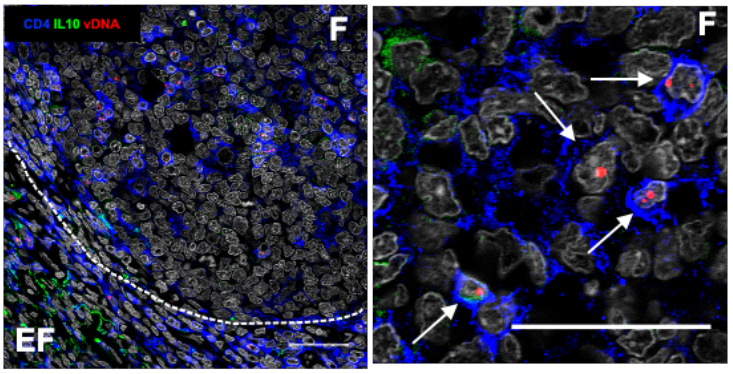
e
CD4 IL10 vDNA
F
EF
F